Approximations to wave scattering by an ice sheet of variable thickness over undulating topography

By D. PORTER[1] AND R. PORTER[2]

[1] Department of Mathematics, University of Reading, P. O. Box 220, Whiteknights, Reading, RG6 6AX, UK.

[2] School of Mathematics, University of Bristol, Bristol, BS8 1TW, UK

(Received 2 December 2003)

An investigation is carried out into the effect on wave propagation of an ice sheet of varying thickness floating on water of varying depth, in three dimensions. By deriving a variational principle equivalent to the governing equations of linear theory and invoking the mild-slope approximation in respect of the ice thickness and water depth variations, a simplified form of the problem is obtained from which the vertical coordinate is absent. Two situations are considered: the scattering of flexural-gravity waves by variations in the thickness of an infinite ice sheet and by depth variations; and the scattering of free surface gravity waves by an ice sheet of finite extent and varying thickness, again incorporating arbitrary topography. Numerical methods are devised for the two-dimensional versions of these problems and a selection of results is presented. The variational approach that is developed can be used to implement more sophisticated approximations and is capable of producing the solution of full linear problems by taking a large enough basis in the Rayleigh-Ritz method. It is also applicable to other situations that involve wave scattering by a floating elastic sheet.

1. Introduction

The effect on surface water waves of a floating elastic plate is of considerable current interest in two particular application areas.

The first of these, and the one on which our approach is focused, is concerned with the way in which the waves interact with thin sheets of sea ice. This issue is particularly important in the Marginal Ice Zone (MIZ) in the Antarctic, a region consisting of loose or packed ice floes that is situated between the ocean and the shore-fast sea ice. As the ice sheets support flexural-gravity waves, the energy carried by ocean waves is capable of propagating far into the MIZ, where it contributes to ice break-up (see Squire *et al.* (1995) for an extensive review). Thin plate, or Kirchhoff, theory has been widely used to model this situation.

Another application area results from a proposal in Japan to build a floating offshore runway, an example of a structure often referred to in the literature as a VLFP (very large floating platform). Again, Kirchhoff theory is used to model the motion of the elastic plate under external loading. Much of the work directed specifically towards this application is either numerical (see, for example, Kashiwagi (1998)) or uses approximation methods, such as the parabolic approximation (Takagi (2002)) or geometric optics (as in Hermans (2003b)).

One of the most significant early attempts at solving problems involving thin elastic

plates on water can be found in Evans & Davies (1968), where the two-dimensional problem of water waves incident upon a semi-infinite thin elastic plate floating on water was solved using the Weiner-Hopf technique. At that time, the solution was only studied in any detail using shallow water theory, although later attempts at this problem, most notably those by Balmforth & Craster (1999), Tkacheva (2001a,b,c) and Linton & Chung (2003), have succeeded in deriving simple expressions for the reflection coefficient in water of both finite and infinite depth.

The problem of two-dimensional water wave scattering by thin elastic plates of finite length has been considered by a number of authors using a variety of different techniques. Thus, for example, a Green's function approach was used by Meylan & Squire (1994) to formulate an integral equation over the plate. In contrast, Newman (1994) developed a general theory for the interaction of water waves with elastic structures. This involved expressing the motion of the structure, considered in isolation, in terms of eigenmodes and identifying a radiation potential to describe the wave response induced by each eigenmode when the structure and fluid motions are coupled. Thus, the full potential for the scattering problem can be written in terms of a superposition of the incident wave potential and an infinity of radiation potentials, in much the same way as the motion of floating rigid bodies can be described by six independent modes. Later, Wu *et al.* (1995) applied the theory of Newman (1994) to a finite length elastic plate and compared their results with experimental data of Utsunomiya *et al.* (1995). Tkacheva (2002) has recently used the Weiner-Hopf technique to formulate a solution for the finite plate in terms of an infinite system of equations, whilst Hermans (2003a) has proposed a method of solution based upon making a particular type of approximation to a function representing the plate deflection, which subsequently appears as the unknown function in an integro-differential equation. Andrianov & Hermans (2003) have also examined scattering by a finite elastic plate for infinite, finite and shallow water depths by deriving an integro-differential equation.

For the more difficult three-dimensional problem, less has been done and attention has generally been focussed on simplified geometries. In particular, wave interaction with a circular elastic plate has been considered by Meylan & Squire (1996), who used Green's identity to formulate an integral equation over the plate and the theory of Newman (1994) to expand the vertical deflection of the plate in term of its *in vacuo* modes. In the case of shallow water, Zilman & Miloh (2000) were able to derive a closed form expression for the solution of this problem. Sturova (2001) has considered more general plate shapes using the shallow water approximation whilst, for the full linearised equations, Meylan (2001) used a variational principle in conjunction with the Rayleigh-Ritz approximation to investigate wave interaction with rectangular plates numerically.

Most of the work described thus far has assumed a plate with non-zero (but small) constant thickness and with zero draught. The latter assumption is often made in order to facilitate analytical progress, although it was relaxed in the work of Wu *et al.* (1995). Very little attention appears to have been paid to the determination of wave scattering by plates of varying thickness. Squire & Dixon (2001) have considered the two-dimensional problem where the entire fluid surface is covered by ice of one constant thickness, with an inclusion of a different constant thickness, although the submergence of each portion of ice is taken to be the same. Hermans (2003b) has used a ray method for a plate of variable thickness, but unfortunately omitted terms from the equation that describes the motion of the plate. The same is true of a later paper by Hermans (2003c) which adopts the solution technique developed in Hermans (2003a), although the method of determining wave scattering by variable thickness in this paper is to replace the variable plate properties by a piecewise constant approximation. In the VLFP context, Takagi *et*

al (2000) used eigenfunction matching to examine the damping effect on flexural waves of a thick block at the edge of an infinite thin sheet and a wide spacing approximation to infer corresponding results for a finite sheet.

The primary aim of the present paper is to develop a model to investigate the effect on wave propagation of an ice sheet of variable thickness. The further generalisation of existing work is made that variations in the topography are also allowed, without introducing an extra level of difficulty. This situation arises because a "vertically integrated" approximation is made to the full linear problem, to reduce the computations to a feasible level. The approximation also gives an overall consistency to the model in the sense that thin plate theory, which is used to model the ice sheet, arises by averaging across the plate and the same process is applied here through the fluid depth.

A starting point is required to implement the approximation and we therefore develop a variational principle that is equivalent to solving the field equation and boundary conditions in the three-dimensional setting. By ensuring that the integrand is the Lagrangian density we are, in effect, using Hamilton's principle which therefore also produces the edge conditions for a plate of varying thickness as natural conditions, without these having to be built explicitly into the derivation.

It is pertinent to mention here that Meylan (2001), in contrast, combined a standard variational principle for the ice sheet (but different from that used in the present work) with a second principle that describes the fluid motion in terms of an inverse operator involving a Green's function. Meylan includes results for plates whose thickness increases linearly but have zero draught, and he evidently does not use the appropriate edge conditions.

Having established a suitable variational principle, the Rayleigh-Ritz approximation can be invoked, that a finite-dimensional approximation to the stationary point of the functional is also an approximation to the solution of its natural conditions. We adopt the simplest approach to approximating wave propagation at this point by using a one-dimensional trial space based on the propagating modes for an ice sheet of constant thickness on water of constant mean depth. The approximation is therefore the counterpart in the present problem of the "mild-slope approximation" for free surface flows over undulating beds devised originally by Berkhoff (1972,1976) and independently by Smith & Sprinks (1975). However, the equations that we derive are extensions of the more recent modified mild-slope equation, derived by Chamberlain & Porter (1995) and re-evaluated in Porter (2003), in which previously neglected curvature terms are shown to be significant.

The effect of using the one-term trial function described is to remove the vertical coordinate from the proceedings, reducing the problem to a pair of coupled partial differential equations in two independent variables that determine the approximations to the fluid motion and the sheet elevation. The variations in the bedform and in the lower surface of the ice sheet appear in the coefficients of the differential equations and it turns out, not surprisingly, that only the difference between these two levels is significant in the approximation to the fluid flow. As indicated earlier, this outcome is consistent with the appearance of the variable ice thickness in the thin plate model.

Approximating the vertical structure of the fluid motion and the consequent elimination of the vertical coordinate is reminiscent of shallow water theory. The mild-slope approximation for free surface motions and its equivalent in the present problem are, in fact, simply generalisations of the shallow water approximation having the advantage that they apply to all wavelengths and not merely to "long waves". Indeed, the shallow water equations are the long wave limits of those based on the mild-slope approximation.

Using our model we develop a solution method for the two-dimensional problem in

which there is complete ice coverage. Here we envisage a flexural-gravity wave incident from infinity upon a region of variable ice thickness and/or undulating topography and determine the main characteristics of the scattered wave field.

To consider the different problem in which an ice floe of variable thickness occupies a finite portion of the water surface, we have to reformulate the variational principle in order to incorporate the free surface regions and the interfaces between these and the region with ice coverage. An illustration of this extension of the theory is again provided in a two dimensional setting, in which a free surface wave is scattered by the ice sheet.

The plan of the paper is as follows. The first main aim is to address the problem in which the surface is completely covered by an ice sheet of variable thickness and the bed has arbitrary undulations. In Section 2 we formulate the problem and in Section 3 derive a variational principle that can be used to generate approximations to it. The approximation described above is developed in Section 4 and it is implemented in Section 5 for a scattering problem in two dimensions. A selection of numerical results is given.

In Section 6 we turn to our second objective by considering the extension of the problem to one in which there is only partial ice cover. Here the various stages in the development and resolution of the original problem are revisited and revised to apply to the extended version, leading again to a sample of computational results.

2. Notation and Formulation

We use cartesian coordinates x, y, z with z directed vertically upwards, $z = 0$ coinciding with the equilibrium position of the free surface of the fluid in the absence of ice. The ice sheet is represented by an elastic plate of constant density ρ_i and varying thickness $D(x, y)$, where D is continuous, which floats in the surface. In equilibrium, the fluid is bounded below by an impermeable fixed bed located at $z = -h(x, y)$, where h is a positive valued, continuous function, and above by the continuous lower surface $z = -d(x, y)$ of the elastic plate.

In motion, the ice sheet undergoes small amplitude flexural oscillations and its lower surface at the horizontal location x, y and time t is given by

$$z = -d(x, y) + \zeta(x, y, t),$$

say, where ζ is an unknown of the problem.

Supposing the fluid to be inviscid, incompressible and homogeneous, its assumed irrotational motion can be described by the velocity potential $\Phi(x, y, z, t)$ satisfying

$$\nabla^2\Phi = 0 \quad (-h < z < -d + \zeta) \tag{2.1}$$

and the bed condition

$$\Phi_z + \nabla_h h.\nabla_h\Phi = 0 \quad (z = -h). \tag{2.2}$$

Here $\nabla = (\partial/\partial x, \partial/\partial y, \partial/\partial z)$, as usual, and $\nabla_h = (\partial/\partial x, \partial/\partial y, 0)$ is its projection onto $z = 0$.

Within the fluid, the linearised version of Bernoulli's equation gives the pressure $p(x, y, z, t)$ in the form

$$p = p_0 - \rho_w\Phi_t - \rho_w gz \quad (-h \le z \le -d), \tag{2.3}$$

in which ρ_w is the density of the water and p_0 denotes the constant atmospheric pressure above the ice sheet.

The motion of the sheet is due to the differential pressure across it and the governing equation may be determined using thin plate theory. Referring to Timoshenko &

Woinowsky-Krieger (1959) we deduce that

$$[p]_{-d+\zeta} = p_0 + \rho_w g d + \rho_w g \mathcal{L}\zeta + \rho_i D \zeta_{tt}, \tag{2.4}$$

where $[\ \ ]_{z_0}$ denotes the value of the included quantity on $z = z_0$ and

$$\mathcal{L}\zeta \equiv \nabla_h^2(\beta \nabla_h^2 \zeta) - (1-\nu)\{\beta_{xx}\zeta_{yy} + \beta_{yy}\zeta_{xx} - 2\beta_{xy}\zeta_{xy}\}.$$

Here ν is Poisson's ratio for ice and

$$\beta(x,y) = F(x,y)/\rho_w g, \quad F(x,y) = ED^3(x,y)/12(1-\nu^2),$$

F being the flexural rigidity of the sheet and E Young's modulus for ice.

The first two terms on the right hand side of (2.4) ensure the equilibrium state of the sheet, as is evident when the equation is combined with (2.3) to couple the ice and fluid motions. Linearising about $z = -d$ on the basis that Φ and ζ are small we find that

$$\rho_w(\Phi_t + g\zeta) + \rho_w g \mathcal{L}\zeta + \rho_i D \zeta_{tt} = 0 \quad (z = -d). \tag{2.5}$$

The further coupling

$$\nabla_h d.\nabla_h \Phi + \Phi_z = \zeta_t \quad (z = -d) \tag{2.6}$$

arises from linearising the kinematic condition $\nabla\Phi.\nabla S + S_t = 0$ applied on the surface $S \equiv z + d - \zeta = 0$. By eliminating ζ between (2.5) and (2.6) we obtain the linearised boundary condition for Φ on the upper fluid surface in the form

$$\begin{aligned}\rho_w\{\Phi_{tt} + g(\nabla_h d.\nabla_h\Phi + \Phi_z)\} + \rho_w g\mathcal{L}(\nabla_h d.\nabla_h\Phi + \Phi_z)\\ +\rho_i D(\nabla_h d.\nabla_h\Phi + \Phi_z)_{tt} = 0 \quad (z = -d).\end{aligned} \tag{2.7}$$

At this point it is convenient to remove a harmonic time dependence by introducing the given angular frequency ω and setting

$$\Phi(x,y,z,t) = \frac{g}{\mathrm{i}\omega}\,\phi(x,y,z)\mathrm{e}^{-\mathrm{i}\omega t}, \quad \zeta(x,y,t) = \eta(x,y)\mathrm{e}^{-\mathrm{i}\omega t},$$

the real parts of which represent the required functions. These substitutions and linearisation transform (2.1) and (2.2) into

$$\nabla^2\phi = 0 \quad (-h < z < -d), \qquad \phi_z + \nabla_h h.\nabla_h\phi = 0 \quad (z = -h), \tag{2.8}$$

whilst (2.5) and (2.6) become

$$(1-\alpha)\eta + \mathcal{L}\eta - \phi = 0, \quad \nabla_h d.\nabla_h\phi + \phi_z = \kappa\eta \quad (z = -d), \tag{2.9}$$

in which we have introduced the quantities

$$\kappa = \omega^2/g, \quad \alpha(x,y) = \kappa\rho_i D(x,y)/\rho_w. \tag{2.10}$$

The time independent counterpart of (2.7) follows most directly by eliminating η from (2.9) to give

$$(1-\alpha)(\nabla_h d.\nabla_h\phi + \phi_z) + \mathcal{L}(\nabla_h d.\nabla_h\phi + \phi_z) = \kappa\phi \quad (z = -d). \tag{2.11}$$

The reduced potential ϕ is therefore determined by (2.8) and (2.11), together with conditions specifying its far-field behaviour as $x^2 + y^2 \to \infty$. This is a formidable proposition except in the case of an ice sheet of constant thickness and a horizontal bed and we therefore seek to approximate the boundary value problem.

3. The variational principle

The approximation is generated by means of a variational principle that is equivalent to the governing equations. The derivation of the principle is most easily carried out by considering the fluid and ice motions separately before coupling them through (2.9).

Let $\mathcal{D}$ denote a simply connected, bounded domain in the plane $z = 0$ with boundary $\mathcal{C}$ on which $\mathbf{n}$ is the outward normal unit vector and let the functions $\psi(x, y, z)$ and $\chi(x, y)$ be sufficiently differentiable for what follows.

We deal first with the equations (2.8) governing the fluid motion and note that the functional

$$L_1(\psi) = \frac{1}{2}\iint_{\mathcal{D}}\int_{-h}^{-d} (\nabla\psi)^2 \,\mathrm{d}z\,\mathrm{d}x\,\mathrm{d}y$$

has first variation

$$\delta L_1 = \iint_{\mathcal{D}}\int_{-h}^{-d} (\nabla.(\delta\psi\nabla\psi) - \delta\psi\nabla^2\psi) \,\mathrm{d}z\,\mathrm{d}x\,\mathrm{d}y.$$

After some manipulation to extricate $\delta\psi$ from the gradient operator, we find that

$$\delta L_1 = \iint_{\mathcal{D}} \Big\{[(\nabla_h d.\nabla_h\psi + \psi_z)\delta\psi]_{-d} - [(\nabla_h h.\nabla_h\psi + \psi_z)\delta\psi]_{-h} - \int_{-h}^{-d} \delta\psi\nabla^2\psi \,\mathrm{d}z\Big\}\,\mathrm{d}x\,\mathrm{d}y + \int_{\mathcal{C}} \mathbf{n}.\int_{-h}^{-d} \delta\psi\nabla_h\psi \,\mathrm{d}z\,\mathrm{d}s, \tag{3.1}$$

where s measures arc length on $\mathcal{C}$.

For the ice sheet the appropriate functional with the coupling term included is

$$L_2(\psi,\chi) = \frac{1}{2}\iint_{\mathcal{D}} \{\beta\{(\nabla_h^2\chi)^2 - 2(1-\nu)(\chi_{xx}\chi_{yy} - \chi_{xy}^2)\} + (1-\alpha)\chi^2 - 2\chi[\psi]_{-d}\}\,\mathrm{d}x\,\mathrm{d}y.$$

The terms involving β represent the strain energy of the sheet, in the form given by Timoshenko & Woinowsky-Krieger (1959). The remaining terms combine the effects of the dynamic pressure on the plate and its acceleration.

The first variation of L_2 is

$$\delta L_2 = \iint_{\mathcal{D}} \{\beta(\nabla_h^2\chi)(\nabla_h^2\delta\chi) - \beta(1-\nu)\{\chi_{xx}\delta\chi_{yy} + \chi_{yy}\delta\chi_{xx} - 2\chi_{xy}\delta\chi_{xy}\} + \{(1-\alpha)\chi - [\psi]_{-d}\}\,\delta\chi - \chi[\delta\psi]_{-d}\}\,\mathrm{d}x\,\mathrm{d}y.$$

To simplify the first term in the integral we use a version of Green's identity, namely,

$$\iint_{\mathcal{D}} \{\beta(\nabla_h^2\chi)(\nabla_h^2\delta\chi) - \delta\chi\nabla_h^2(\beta\nabla_h^2\chi)\}\,\mathrm{d}x\,\mathrm{d}y = \int_{\mathcal{C}} \Big\{\beta\nabla_h^2\chi\frac{\partial}{\partial n}(\delta\chi) - \delta\chi\frac{\partial}{\partial n}(\beta\nabla_h^2\chi)\Big\}\,\mathrm{d}s,$$

where $\partial/\partial n = \mathbf{n}.\nabla_h$. Domain and boundary contributions can similarly be distinguished for the other term in δL_2 involving β, since

$$\beta\{\chi_{xx}\delta\chi_{yy} + \chi_{yy}\delta\chi_{xx} - 2\chi_{xy}\delta\chi_{xy}\} = \delta\chi(\beta_{xx}\zeta_{yy} + \beta_{yy}\zeta_{xx} - 2\beta_{xy}\zeta_{xy}) + \nabla_h.\mathbf{c},$$

in which

$$\mathbf{c} = \{\beta(\chi_{yy}\delta\chi_x - \chi_{xy}\delta\chi_y) - (\beta_x\chi_{yy} - \beta_y\chi_{xy})\delta\chi\}\mathbf{i} + \{\beta(\chi_{xx}\delta\chi_y - \chi_{xy}\delta\chi_x) - (\beta_y\chi_{xx} - \beta_x\chi_{xy})\delta\chi\}\mathbf{j},$$

the unit vectors having their usual meanings. These identities allow δL_2 to be rearranged

as

$$\delta L_2 = \iint_{\mathcal{D}} \Big\{ \{(1-\alpha)\chi + \mathcal{L}\chi - [\psi]_{-d}\}\delta\chi - \chi[\delta\psi]_{-d} \Big\}\, \mathrm{d}x\, \mathrm{d}y + \int_{\mathcal{C}} \Big\{ \beta\nabla_h^2\chi \frac{\partial}{\partial n}(\delta\chi) - \delta\chi \frac{\partial}{\partial n}(\beta\nabla_h^2\chi) - (1-\nu)\mathbf{n}.\mathbf{c} \Big\}\, \mathrm{d}s. \tag{3.2}$$

We now form the functional $L_{\mathcal{D}} \equiv L_1 + \kappa L_2$, that is,

$$L_{\mathcal{D}}(\psi,\chi) = \frac{1}{2}\iint_{\mathcal{D}} \Big\{ \int_{-h}^{-d} (\nabla\psi)^2\, \mathrm{d}z - 2\kappa\beta(1-\nu)(\chi_{xx}\chi_{yy} - \chi_{xy}^2) + \kappa\{(1-\alpha)\chi^2 + \beta(\nabla_h^2\chi)^2 - 2\chi[\psi]_{-d}\} \Big\}\, \mathrm{d}x\, \mathrm{d}y \tag{3.3}$$

and we also assume the variations to be such that

$$\delta\psi = 0 \ \text{ on } \ \mathcal{C}\times[-h,-d], \quad \delta\chi = \delta\chi_x = \delta\chi_y = 0 \ \text{ on } \ \mathcal{C}. \tag{3.4}$$

This simplification is possible as our first aim is to approximate the vertical structure of the motion and not to deal with conditions on lateral boundaries.

It therefore follows from (3.1) and (3.2) that

$$\delta L_{\mathcal{D}} = \iint_{\mathcal{D}} \Big\{ [(\nabla_h d.\nabla_h\psi + \psi_z - \kappa\chi)\delta\psi]_{-d} - [(\nabla_h h.\nabla_h\psi + \psi_z)\delta\psi]_{-h} + \kappa\{(1-\alpha)\chi + \mathcal{L}\chi - [\psi]_{-d}\}\ \delta\chi - \int_{-h}^{-d} \delta\psi\ \nabla^2\psi\ \mathrm{d}z \Big\}\, \mathrm{d}x\, \mathrm{d}y, \tag{3.5}$$

from which we can immediately deduce that $\delta L_{\mathcal{D}} = 0$ at $\psi = \phi$, $\chi = \eta$ for arbitrary variations $\delta\psi$ and $\delta\chi$ satisfying (3.4) if and only if ϕ and η satisfy (2.8) and (2.9). This outcome is not surprising as we have in effect applied Hamilton's principle to the problem.

Finding the stationary point (ϕ,η) of $L_{\mathcal{D}}(\psi,\chi)$ is therefore equivalent to solving (2.8) and (2.9) and approximate solutions of those equations are obtained by approximating the stationary point of $L_{\mathcal{D}}$.

Imposing the second of the natural conditions (2.9) as a constraint, by substituting $\chi = \kappa^{-1}(\nabla_h d.\nabla_h\psi + \psi_z)$ into $L_{\mathcal{D}}(\psi,\chi)$, defines the functional $\widetilde{L}_{\mathcal{D}}(\psi)$, say, and the natural conditions of $\delta\widetilde{L}_{\mathcal{D}} = 0$ will of course be (2.8) and (2.11). It is much more straightforward, however, to use $L_{\mathcal{D}}(\psi,\chi)$ as it stands.

3.1. *Jump conditions*

We can exploit the variational principle further by deriving the natural conditions that apply at an internal boundary of $\mathcal{D}$. This aspect is significant in relation to the approximation developed in the next section and to the case of partial ice cover considered later.

Suppose then that the smooth, simple curve Γ divides $\mathcal{D}$ into two domains $\mathcal{D}_+$ and $\mathcal{D}_-$, say. The principle $\delta(L_{\mathcal{D}_+} + L_{\mathcal{D}_-}) = 0$ subject to (3.4) gives (2.8) and (2.9) for $(x,y) \in \mathcal{D}_\pm$ and, in addition, natural conditions at the interface. Let $\langle\chi\rangle = \chi_+ - \chi_-$ denote the jump in χ across Γ and $\langle\langle\psi\rangle\rangle = \psi_+ - \psi_-$ the jump in ψ across the surface $\Gamma\times[-h,-d]$, the subscripts denoting the limiting values of the functions from $\mathcal{D}_\pm$.

We deduce from (3.1) and (3.2) that the contribution to $\delta(L_{\mathcal{D}_+} + L_{\mathcal{D}_-})$ on Γ is

$$C_\Gamma = \int_\Gamma \mathbf{n}.\Big\langle \int_{-h}^{-d} \delta\psi\nabla_h\psi\ \mathrm{d}z + (\beta\nabla_h^2\chi)\nabla_h(\delta\chi) - \delta\chi\nabla_h(\beta\nabla_h^2\chi) - (1-\nu)\mathbf{c} \Big\rangle\, \mathrm{d}s. \tag{3.6}$$

We have carried over the notation adopted for the external boundary of $\mathcal{D}$ to its internal

boundary, by using s to denote arc length on Γ and $\mathbf{n}$ the unit normal vector on the curve, chosen here so that it is directed from $\mathcal{D}_+$ to $\mathcal{D}_-$.

To identify the natural conditions implied by $C_\Gamma = 0$ it is necessary to transform to boundary coordinates. Let $\mathbf{n}$ have direction cosines $(\cos\theta, \sin\theta, 0)$ with respect to the fixed cartesian frame, where $\theta = \theta(s)$, and introduce the unit vector $\mathbf{s}$ tangential to Γ, orientated so that

$$\mathbf{n} = \mathbf{i}\cos\theta + \mathbf{j}\sin\theta, \quad \mathbf{s} = -\mathbf{i}\sin\theta + \mathbf{j}\cos\theta.$$

A straightforward transformation then gives

$$\mathbf{n}.\mathbf{c} = (\chi_{ss} + \theta'\chi_n)(\beta\delta\chi_n - \beta_n\delta\chi) - (\chi_{ns} - \theta'\chi_s)(\beta\delta\chi_s - \beta_s\delta\chi),$$

where $\partial/\partial s = \mathbf{s}.\nabla_h$. Therefore

$$C_\Gamma = \int_\Gamma \Big\langle \int_{-h}^{-d} \delta\psi\ \mathbf{n}.\nabla_h\psi\ \mathrm{d}z + (\beta\nabla_h^2\chi)\delta\chi_n - \delta\chi(\beta\nabla_h^2\chi)_n \\ -(1-\nu)\{(\chi_{ss} + \theta'\chi_n)(\beta\delta\chi_n - \beta_n\delta\chi) - (\chi_{ns} - \theta'\chi_s)(\beta\delta\chi_s - \beta_s\delta\chi)\}\Big\rangle\ \mathrm{d}s.$$

The net term in $\delta\chi$ is obtained after an integration by parts to remove $\delta\chi_s$.

Thus, if we impose the essential conditions that ψ, χ and χ_n are continuous across Γ we infer that

$$\langle\!\langle \mathbf{n}.\nabla_h\phi \rangle\!\rangle = \langle \mathcal{M}\eta \rangle = \langle \mathcal{S}\eta \rangle = 0 \tag{3.7}$$

are the natural jump conditions satisfied by the solutions $\psi = \phi$ and $\chi = \eta$ of $\delta(L_{\mathcal{D}_+} + L_{\mathcal{D}_-}) = 0$, where

$$\left.\begin{aligned} \mathcal{M}\eta &\equiv \nabla_h^2\eta - (1-\nu)(\eta_{ss} + \theta'\eta_n), \\ \mathcal{S}\eta &\equiv (\beta\nabla_h^2\eta)_n - (1-\nu)\{(\eta_{ss} + \theta'\eta_n)\beta_n \\ &\qquad -2(\eta_{ns} - \theta'\eta_s)\beta_s - (\eta_{ns} - \theta'\eta_s)_s\beta\}. \end{aligned}\right\}$$

In addition, the integration by parts referred to above gives the natural condition

$$\eta_{ns} - \theta'\eta_s \equiv \eta_{sn} = 0$$

at every end of Γ, assuming that $D \neq 0$ there, the identity being a property of the boundary coordinates that is easily established.

The conditions (3.7) respectively represent continuity of the horizontal fluid velocity and continuity of bending moment and shear stress in the ice sheet. Continuity of fluid pressure and of ice sheet displacement and velocity are guaranteed by the essential conditions, which imply that $\langle\!\langle\phi\rangle\!\rangle = \langle\eta\rangle = \langle\eta_n\rangle = 0$. The continuity conditions for the ice sheet that we have derived are closely related to edge conditions prevailing at a vertical crack in the ice sheet along Γ, for example, which have been given by Sturova (2001) in the case of constant ice thickness. Although we have so far assumed that D is continuous, the formulation given effectively incorporates the case where Γ is the location of a thin crack. It is, of course, inevitable that a variational principle which embodies the dynamics of the problem appropriately will give all of the relevant conditions.

We remark at this point that, as the governing equations have real-valued coefficients, we have used real-valued functionals to form the variational principle. The inclusion of radiation conditions for complex harmonic waves in the set of natural conditions, say, requires different functionals. Thus the integrand of $L_1(\psi)$ would have to be modified to $\nabla\psi.\nabla\overline{\psi}$ to include radiation conditions, with corresponding changes in L_2. This aspect does not concern us in the present work.

4. An approximation

Our objective is to reduce the dimension of the boundary value problem by approximating the dependence of ϕ on z. This is achieved by basing the vertical fluid motion on that for a horizontal bed and an ice sheet of uniform thickness.

To establish the approximation we therefore consider a horizontal bed at $z = -h_0$ and let the ice sheet have constant thickness D_0 with its horizontal lower face at the equilibrium level $z = -d_0$. Correspondingly, α and β take the constant values α_0 and β_0, respectively. In this reduced problem, (2.8) becomes

$$\nabla^2\phi = 0 \quad (-h_0 < z < -d_0), \qquad \phi_z = 0 \quad (z = -h_0), \tag{4.1}$$

and (2.9) takes the form

$$(1 - \alpha_0 + \beta_0\nabla_h^4)\eta - \phi = 0, \quad \phi_z = \kappa\eta \quad (z = -d_0).$$

These equations imply the simplified version

$$(1 - \alpha_0 + \beta_0\nabla_h^4)\phi_z = \kappa\phi \quad (z = -d_0) \tag{4.2}$$

of (2.11). It is easy to show that propagating plane wave solutions of (4.1) and (4.2) with crests parallel to the y axis are

$$\phi_p^{\pm}(x, z) = \mathrm{e}^{\pm \mathrm{i}k_0 x}\cosh k_0(z + h_0), \tag{4.3}$$

where $k = \pm k_0$ are the only real roots of the dispersion relation

$$(1 - \alpha_0 + \beta_0 k^4)k\tanh k(h_0 - d_0) = \kappa. \tag{4.4}$$

This equation also has roots corresponding to evanescent modes, namely, four complex roots symmetrically placed with respect to both the real and imaginary axes and infinitely many purely imaginary roots.

We can use this information to approximate ϕ and η in the case of varying h, d and D in a number of ways. The simplest is to set

$$\left.\begin{aligned} \phi(x, y, z) \approx \psi(x, y, z) = \varphi(x, y)w(x, y, z), \\ w(x, y, z) = \operatorname{sech} k(h - d)\cosh k(z + h), \end{aligned}\right\} \tag{4.5}$$

where $k = k(x, y)$ denotes the positive real root of

$$(1 - \alpha + \beta k^4)k\tanh k(h - d) = \kappa \tag{4.6}$$

with $h = h(x, y)$, $d = d(x, y)$ and $D = D(x, y)$. Because the dependence of ψ on z is locally that in (4.3) we expect to approximate waves that propagate beneath the ice sheet and are modulated by its varying thickness and the undulating bedform. We note that the scaling $w(x, y, -d) = 1$ has been chosen for convenience and that η is only approximated indirectly.

The assumption underlying the approximation is that the perturbations about $h = h_0$, $d = d_0$ and $D = D_0$ are slowly-varying functions, that is,

$$|\nabla_h h| \ll kh, \quad |\nabla_h d| \ll kd, \quad |\nabla_h D| \ll kD,$$

for all relevant values of x, y.

To implement the approximation (4.5) we substitute it into $L(\psi, \chi)$ and enforce $\delta L = 0$, noting that $\delta\psi = w\delta\varphi$. It follows from (3.5) that L is stationary with respect to arbitrary variations $\delta\varphi$ and $\delta\chi$ satisfying (3.4) (so that $\delta\varphi = 0$ on $\mathcal{C}$), provided that

$$[w\{\nabla_h d.\nabla_h(w\varphi) + w_z\varphi - \kappa\chi\}]_{-d} - [w\nabla_h h.\nabla_h(w\varphi)]_{-h} - \int_{-h}^{-d} w\nabla^2(w\varphi)\,\mathrm{d}z = 0$$

and

$$(1-\alpha)\chi + \mathcal{L}\chi - [w]_{-d}\varphi = 0,$$

in which $[w_z]_{-h} = 0$ has been used. Rearranging the first of these equations by means of the identity

$$\int_{-h}^{-d} w\nabla_h^2(w\varphi)\ \mathrm{d}z = [w\nabla_h d.\nabla_h(w\varphi)]_{-d} - [w\nabla_h h.\nabla_h(w\varphi)]_{-h} + \nabla_h.\int_{-h}^{-d} w^2\nabla_h\varphi\ \mathrm{d}z + \Big\{\nabla_h.\int_{-h}^{-d} w\nabla_h w\ \mathrm{d}z - \int_{-h}^{-d}(\nabla_h w)^2\ \mathrm{d}z\Big\}\varphi,$$

and applying the normalisation $[w]_{-d} = 1$, we deduce the pair of formally self-adjoint coupled equations

$$\left.\begin{aligned} \nabla_h.a\nabla_h\varphi + b\varphi + \kappa\chi = 0, \\ (1-\alpha)\chi + \mathcal{L}\chi - \varphi = 0, \end{aligned}\right\} \tag{4.7}$$

in which

$$\left.\begin{aligned} a = \int_{-h}^{-d} w^2\ \mathrm{d}z = (4k)^{-1}\mathrm{sech}^2 k(h-d)\{2k(h-d) + \sinh 2k(h-d)\}, \\ b = k^2 a - k\tanh k(h-d) + \nabla_h.\int_{-h}^{-d} w\nabla_h w\ \mathrm{d}z - \int_{-h}^{-d}(\nabla_h w)^2\ \mathrm{d}z. \end{aligned}\right\} \tag{4.8}$$

Thus the approximations $\phi \approx w\varphi$ and $\eta \approx \chi$ are determined by solving (4.7).

Alternatively, the equation

$$(1-\alpha+\mathcal{L})(\nabla_h.a\nabla_h + b)\varphi + \kappa\varphi = 0, \tag{4.9}$$

which follows by eliminating χ from (4.7), can be solved and χ recovered from (4.7). It is inevitable that the approximation (4.5) will lead to a sixth order differential equation for φ, as the effect of integrating out the variable z in the application of the variational principle is to convert Laplace's equation into a second order equation for φ and merge this with the boundary conditions on $z = -h$ and $z = -d$ and, in particular, with the fourth order condition on $z = -d$.

We note here that the shallow water approximation $kh \ll 1$ corresponds to making the different choice $w = 1$ in (4.5), which ensures that the horizontal velocity field $\nabla_h\phi \approx \nabla_h\psi$ is independent of z, as the approximation requires. Thus, putting $\phi \approx \psi = \varphi$ in the variational principle $\delta L_{\mathcal{D}} = 0$ we arrive at

$$\nabla_h.(h-d)\nabla_h\varphi + \kappa\chi = 0, \quad (1-\alpha)\chi + \mathcal{L}\chi - \varphi = 0. \tag{4.10}$$

The equations (4.7) may be regarded as the extension of the shallow water approximation to general values of kh and, as we would expect, they reduce to (4.10) in the shallow water limit.

For practical purposes the coefficients in the first equation of (4.7) must be converted into a more explicit form. This can be achieved by first introducing the variables

$$Z = z + d, \quad H = h - d, \tag{4.11}$$

so that, by (4.6), $k = k(H, D)$ and from (4.5)

$$w(x, y, z) \equiv W(H, D, Z) = \mathrm{sech}\,(kH)\cosh k(Z+H) \quad (-H \le Z \le 0). \tag{4.12}$$

Thus $\nabla_h w = \nabla_h W = W_H\nabla_h H + W_D\nabla_h D$, where $W_H = \partial W/\partial H$ and similarly for W_D.

Using this expansion, the second element of (4.8) can be written as

$$\left.\begin{aligned} b = k^2 a - k\tanh(kH) + (W, W_H)\nabla_h^2 H + (W, W_D)\nabla_h^2 D \\ +C^{(1)}(\nabla_h H)^2 + C^{(2)}(\nabla_h D)^2 + C^{(3)}\nabla_h H.\nabla_h D, \end{aligned}\right\} \tag{4.13}$$

in which

$$\left.\begin{aligned} C^{(1)} = (W, W_H)_H - ||W_H||^2, \quad C^{(2)} = (W, W_D)_D - ||W_D||^2, \\ C^{(3)} = (W, W_H)_D + (W, W_D)_H - 2(W_H, W_D), \end{aligned}\right\} \tag{4.14}$$

and the inner product notation

$$(u, v) = \int_{-H}^{0} u\overline{v}, \quad ||u||^2 = (u, u)$$

has been introduced for brevity.

The equations (4.7) hold only in domains where h, d and D are differentiable and they have to be replaced by equivalent jump conditions where this is not the case. We suppose that φ, χ and $\nabla_h\chi$ are continuous everywhere, in accordance with the essential conditions applied in the derivation of (3.7), and that $\nabla_h h$, $\nabla_h d$ and $\nabla_h D$ are discontinuous along a smooth, simple curve Γ in the x, y plane. It follows by using $\psi = \varphi w$ in (3.6) and applying (4.11) to simplify the result that the most general jump conditions on Γ are

$$\left.\begin{aligned} a\langle \mathbf{n}.\nabla_h\varphi\rangle + \langle \mathbf{n}.\{(W, W_H)\nabla_h H + (W, W_D)\nabla_h D\}\rangle\varphi = 0, \\ \langle \mathcal{M}\chi\rangle = \langle \mathcal{S}\chi\rangle = 0, \end{aligned}\right\} \tag{4.15}$$

where we have adopted the notation used in (3.7).

By enforcing $\langle\varphi\rangle = \langle\chi\rangle = \langle \mathbf{n}.\nabla_h\chi\rangle = 0$ we have imposed continuity of pressure across $\Gamma \times [-h, -d]$ and of ice sheet displacement and velocity across Γ, and the natural conditions (4.15) resulting from the variational principle are the counterparts of (3.7) for the approximate solution. The first represents conservation of energy flux across $\Gamma \times [-h, -d]$, aggregated over the depth, and the other two show that the bending moment and shear stress of the ice sheet are conserved across Γ, as they are in the exact solution.

5. Two-dimensional scattering

We illustrate the approximation by applying it in a two-dimensional context where $h = h(x)$, $d = d(x)$, $D = D(x)$ and the motion is independent of y. In this case (4.7) reduces to

$$(a(x)\varphi')' + b(x)\varphi + \kappa\chi = 0, \quad (\beta(x)\chi'')'' + (1 - \alpha(x))\chi - \varphi = 0,$$

which can be written as the second order system

$$\left.\begin{aligned} (a(x)\phi_0')' + b(x)\phi_0 + \kappa\phi_1 = 0, \\ \beta(x)\phi_1'' - \phi_2 = 0, \\ \phi_2'' + (1 - \alpha(x))\phi_1 - \phi_0 = 0, \end{aligned}\right\} \tag{5.1}$$

where $\phi_0 = \varphi$, $\phi_1 = \chi$ and $\phi_2 = \beta\chi''$ is the bending moment. In this framework, the jump conditions (4.15) and the associated continuity hypotheses imply that

$$\left.\begin{aligned} a\langle\phi_0'\rangle + \langle(W, W_H)H' + (W, W_D)D'\rangle\phi_0 = 0, \\ \langle\phi_0\rangle = \langle\phi_1\rangle = \langle\phi_2\rangle = \langle\phi_1'\rangle = \langle\phi_2'\rangle = 0, \end{aligned}\right\} \tag{5.2}$$

hold where at least one of $H = h - d$ and D has a slope discontinuity.

The first step is to determine the solutions of (5.1) for constant values of h, d and D. Suppose that $h = h_0$, $d = d_0$ and $D = D_0$ with the values of other quantities denoted in the same way. For this purpose we can return to (4.9) in the reduced form

$$\{\beta_0(\mathrm{d}/\mathrm{d}x)^4 + 1 - \alpha_0\}\{a_0(\mathrm{d}/\mathrm{d}x)^2 + k_0^2 a_0 - k_0 \tanh(k_0 H_0)\}\varphi + \kappa\varphi = 0$$

(where $H_0 = h_0 - d_0$). If we seek solutions $\varphi(x) = \exp(\mathrm{i}\mu x)$, we find that μ is determined by

$$(\beta_0\mu^4 + 1 - \alpha_0)\{a_0(\mu^2 - k_0^2) + k_0 \tanh(k_0 H_0)\} = \kappa, \tag{5.3}$$

from which κ can be eliminated using (4.4) to give

$$(\mu^2 - k_0^2)\{a_0(\beta_0\mu^4 + 1 - \alpha_0) + \beta_0(\mu^2 + k_0^2)k_0 \tanh(k_0 H_0)\} = 0. \tag{5.4}$$

Thus two roots are $\mu = \pm k_0$, as expected, and we recover the propagating waves referred to earlier.

It is easily shown using (4.8) that the other four roots of (5.4) can be written in the forms $\mu = \pm\mu_0$ and $\mu = \pm\overline{\mu}_0$, where $\mu_0 = p_0 + \mathrm{i}q_0$. Here, p_0 and q_0 are positive for all parameter values and are given by setting $h = h_0$ and so on in the expressions

$$\left.\begin{gathered} p = (\lambda_1^2 + \lambda_2^2)^{1/4}\sin(\theta/2), \quad q = (\lambda_1^2 + \lambda_2^2)^{1/4}\cos(\theta/2), \\ \lambda_1 = k\tanh(K)/2a, \quad \lambda_2^2 = (1-\alpha)/\beta + k^4\{1 - 4K^2/(2K + \sinh(2K))^2\}, \\ \theta = \tan^{-1}(\lambda_2/\lambda_1), \quad K = kH. \end{gathered}\right\}$$

These roots are not the complex roots of (4.4) as they are not associated with the correct depth dependence, but they may be regarded as approximations to those roots in the sense that they have the same form but have compensated for the fixed depth function w. To include the exact evanescent modes corresponding to the complex roots of (4.4) requires the use of a three term approximation at the outset in place of (4.5), and this leads to three coupled sixth order equations.

We also remark that in the shallow water case, where a_0 is approximated by H_0, (5.3) reduces to

$$(\beta_0\mu^4 + 1 - \alpha_0)\mu^2 H_0 = \kappa,$$

which is the shallow water limit of the dispersion relation (4.4). The four complex roots are therefore exact in this case, but this is to be expected as the vertical fluid motion is approximated by taking $w = 1$ and, unlike (4.5), does not select a particular mode.

5.1. *A particular problem*

We now assume that the continuous functions $h(x)$, $d(x)$ and $D(x)$ are such that

$$\left.\begin{aligned} h(x) = h_0, \quad d(x) = d_0, \quad D(x) = D_0 \quad (x < 0) \\ h(x) = h_1, \quad d(x) = d_1, \quad D(x) = D_1 \quad (x > \ell) \end{aligned}\right\},$$

where h_i, d_i and D_i are constants for $i = 0, 1$. For simplicity, we suppose that $h'(x)$, $d'(x)$ and $D'(x)$ are continuous for $0 < x < \ell$ but allow for discontinuities in these functions at $x = 0$ and $x = \ell$.

We have established that the propagating waves with $h = h_0$, $d = d_0$ and $D = D_0$ are $\exp(\pm\mathrm{i}k_0 x)$, k_0 being the real, positive root of (5.4). We denote by $\exp(\pm\mathrm{i}k_1 x)$ the propagating waves in $x > \ell$ and we shall similarly attach the subscript 1 to other quantities to indicate that they are to be evaluated for $h = h_1$, $d = d_1$ and $D = D_1$. We

therefore seek solutions for $\phi_0 = \varphi$ that satisfy

$$\phi_0 \sim \left\{ \begin{array}{ll} A_0 \mathrm{e}^{\mathrm{i}k_0 x} + B_0 \mathrm{e}^{-\mathrm{i}k_0 x} & (x \to -\infty), \\ A_1 \mathrm{e}^{\mathrm{i}k_1(\ell - x)} + B_1 \mathrm{e}^{-\mathrm{i}k_1(\ell - x)} & (x \to \infty), \end{array} \right\} \tag{5.5}$$

in which A_0 and $A_1 \exp(\mathrm{i}k_1\ell)$ are respectively the amplitudes of incident waves from the left and right and B_0 and $B_1 \exp(-\mathrm{i}k_1\ell)$ are the amplitudes of the waves scattered to the left and right, respectively. The scattering process may be summarised in the equation

$$\left(\begin{array}{c} B_0 \\ B_1 \end{array} \right) = S \left(\begin{array}{c} A_0 \\ A_1 \end{array} \right) \quad S = \left(\begin{array}{cc} R_0 & T_1 \\ T_0 & R_1 \end{array} \right), \tag{5.6}$$

where R_i and T_i are (to within known phase factors) the complex amplitudes of the reflected and transmitted waves resulting from an incident wave of unit amplitude from $x < 0$ $(i = 0)$ and $x > \ell$ $(i = 1)$. We remark that the far-field for the approximation to full velocity potential $\phi(x, z)$ corresponding to (5.5), that is,

$$\phi \sim \left\{ \begin{array}{ll} \{A_0 \mathrm{e}^{\mathrm{i}k_0 x} + B_0 \mathrm{e}^{-\mathrm{i}k_0 x}\} w_0(x, z) & (x \to -\infty), \\ \{A_1 \mathrm{e}^{\mathrm{i}k_1(\ell - x)} + B_1 \mathrm{e}^{-\mathrm{i}k_1(\ell - x)}\} w_1(x, z) & (x \to \infty), \end{array} \right. \tag{5.7}$$

has the form of the exact solution.

Expressing (5.1) in matrix form, we have to determine the solution of

$$(U\boldsymbol{\Phi}')' = V\boldsymbol{\Phi}, \quad \boldsymbol{\Phi} = (\phi_0, \phi_1, \phi_2)^T, \tag{5.8}$$

which is continuous everywhere, with

$$U = \left(\begin{array}{ccc} a & 0 & 0 \\ 0 & 1 & 0 \\ 0 & 0 & 1 \end{array} \right), \quad V = \left(\begin{array}{ccc} -b & -\kappa & 0 \\ 0 & 0 & \beta^{-1} \\ 1 & \alpha - 1 & 0 \end{array} \right). \tag{5.9}$$

The differential equations may in turn be written as the first order system

$$\left(\begin{array}{c} \boldsymbol{\Phi} \\ U\boldsymbol{\Phi}' \end{array} \right)' = \left(\begin{array}{cc} 0 & U^{-1} \\ V & 0 \end{array} \right) \left(\begin{array}{c} \boldsymbol{\Phi} \\ U\boldsymbol{\Phi}' \end{array} \right), \tag{5.10}$$

in which $U\boldsymbol{\Phi}'$ is now regarded as a dependent variable.

To obtain a boundary value problem for (5.10) with $0 < x < \ell$ we make use of the solutions in the two regions with h, d and D constant. Now ϕ_0 in this case is a linear combination of $\exp(\pm\mathrm{i}k_i x)$, $\exp(\pm\mathrm{i}\mu_i x)$ and $\exp(\pm\mathrm{i}\overline{\mu}_i x)$ (where $i = 0$ for $x < 0$, $i = 1$ for $x > \ell$). It follows from (5.1) that a complete set of linearly independent solutions of (5.8) in the domains where h, d and D are constant is

$$\mathbf{c}_i(k_i)\mathrm{e}^{\pm\mathrm{i}k_i x}, \quad \mathbf{c}_i(\mu_i)\mathrm{e}^{\pm\mathrm{i}\mu_i x}, \quad \mathbf{c}_i(\overline{\mu}_i)\mathrm{e}^{\pm\mathrm{i}\overline{\mu}_i x}, \tag{5.11}$$

with

$$\mathbf{c}_i(u) = (1, \kappa^{-1}(a_i u^2 - b_i), -\kappa^{-1}\beta_i u^2 (a_i u^2 - b_i))^T.$$

The appropriate solution for $x < 0$ can therefore be written as

$$\boldsymbol{\Phi}(x) = C_0(A_0 \mathrm{e}^{\mathrm{i}k_0 x}, 0, 0)^T + C_0(B_0 \mathrm{e}^{-\mathrm{i}k_0 x}, B_0^{(1)} \mathrm{e}^{-\mathrm{i}\mu_0 x}, B_0^{(2)} \mathrm{e}^{\mathrm{i}\overline{\mu}_0 x})^T, \tag{5.12}$$

which incorporates (5.5) and in which $B_0^{(1)}$ and $B_0^{(2)}$ are the unknown complex amplitudes of evanescent modes. C_0 denotes the 3×3 matrix given by setting $i = 0$ in

$$C_i = (\mathbf{c}_i(k_i), \mathbf{c}_i(\mu_i), \mathbf{c}_i(\overline{\mu}_i)).$$

We deduce from (5.12) that

$$\mathbf{\Phi}(0-) = C_0\mathbf{A}_0 + C_0\mathbf{B}_0, \quad \mathbf{A}_0 = (A_0, 0, 0)^T, \quad \mathbf{B}_0 = (B_0, B_0^{(1)}, B_0^{(2)})^T,$$

and that

$$\mathbf{\Phi}'(0-) = \mathrm{i}C_0\mathcal{K}_0\mathbf{A}_0 - \mathrm{i}C_0\mathcal{K}_0\mathbf{B}_0,$$

in which $\mathcal{K}_i$ is the 3×3 matrix given by $\mathcal{K}_i = \mathrm{diag}(k_i, \mu_i, -\overline{\mu}_i)$. Therefore

$$\left.\begin{aligned} C_0^{-1}\mathbf{\Phi}'(0-) + \mathrm{i}\mathcal{K}_0C_0^{-1}\mathbf{\Phi}(0-) &= 2\mathrm{i}\mathcal{K}_0\mathbf{A}_0, \\ C_0^{-1}\mathbf{\Phi}'(0-) - \mathrm{i}\mathcal{K}_0C_0^{-1}\mathbf{\Phi}(0-) &= -2\mathrm{i}\mathcal{K}_0\mathbf{B}_0. \end{aligned}\right\} \tag{5.13}$$

We infer from (5.2) that

$$a_0\{\phi_0'(0-) - \phi_0'(0+)\} = j_0\phi_0(0), \quad \phi_1'(0-) = \phi_1'(0+), \quad \phi_2'(0-) = \phi_2'(0+),$$

where

$$j_0 = (W, W_H)H'(0+) + (W, W_D)D'(0+), \tag{5.14}$$

(with $H = h - d$) which implies that

$$U_0\{\mathbf{\Phi}'(0-) - \mathbf{\Phi}'(0+)\} = J_0\mathbf{\Phi}(0-) = J_0\mathbf{\Phi}(0+), \quad J_i = \mathrm{diag}(j_i, 0, 0).$$

Combining this jump condition with (5.13) we obtain

$$P_0\begin{pmatrix} \mathbf{\Phi}(0+) \\ U_0\mathbf{\Phi}'(0+) \end{pmatrix} = 2\mathrm{i}\mathcal{K}_0\mathbf{A}_0, \quad Q_0\begin{pmatrix} \mathbf{\Phi}(0+) \\ U_0\mathbf{\Phi}'(0+) \end{pmatrix} = -2\mathrm{i}\mathcal{K}_0\mathbf{B}_0, \tag{5.15}$$

in which the 3×6 matrices P_i and Q_i are given by

$$P_i = \Big(C_i^{-1}U_i^{-1}J_i + \mathrm{i}\mathcal{K}_iC_i^{-1}, \;\; C_i^{-1}U_i^{-1}\Big), \quad Q_i = \Big(C_i^{-1}U_i^{-1}J_i - \mathrm{i}\mathcal{K}_iC_i^{-1}, \;\; C_i^{-1}U_i^{-1}\Big).$$

For $x > \ell$ we take

$$\mathbf{\Phi}(x) = C_1(A_1\mathrm{e}^{\mathrm{i}k_1(\ell-x)}, 0, 0)^T + C_1(B_1\mathrm{e}^{-\mathrm{i}k_1(\ell-x)}, B_1^{(1)}\mathrm{e}^{-\mathrm{i}\mu_1(\ell-x)}, B_1^{(2)}\mathrm{e}^{\mathrm{i}\overline{\mu}_1(\ell-x)})^T, \tag{5.16}$$

in accordance with (5.5), $B_1^{(i)}$ $(i = 1, 2)$ being unknown evanescent wave amplitudes, and this leads to

$$Q_1\begin{pmatrix} \mathbf{\Phi}(\ell-) \\ U_1\mathbf{\Phi}'(\ell-) \end{pmatrix} = -2\mathrm{i}\mathcal{K}_1\mathbf{A}_1, \quad P_1\begin{pmatrix} \mathbf{\Phi}(\ell-) \\ U_1\mathbf{\Phi}'(\ell-) \end{pmatrix} = 2\mathrm{i}\mathcal{K}_1\mathbf{B}_1, \tag{5.17}$$

where

$$\mathbf{A}_1 = (A_1, 0, 0)^T, \quad \mathbf{B}_1 = (B_1, B_1^{(1)}, B_1^{(2)})$$

and we have introduced

$$j_1 = (W, W_H)H'(\ell-) + (W, W_D)D'(\ell-)$$

to parallel (5.14).

Recalling that the vectors $\mathbf{A}_i$ contain only the notionally assigned amplitudes A_i, we see that the first element of each of (5.15) and (5.17) is a boundary condition for (5.10); the second elements determine the scattered wave amplitudes contained in the vectors $\mathbf{B}_i$ once the solution of (5.10) is known for $0 \le x \le \ell$.

Suppose that $\mathbf{\Psi}^{(i)}$ $(i = 1, \ldots, 6)$ denote six linearly independent solutions of (5.10) in this interval, obtained by solving initial value problems. Then the general solution of (5.10) for $0 \le x \le \ell$ may be written as

$$\begin{pmatrix} \mathbf{\Phi}(x) \\ U(x)\mathbf{\Phi}'(x) \end{pmatrix} = \Psi(x)\mathbf{E}, \quad \Psi = (\mathbf{\Psi}^{(1)}, \ldots, \mathbf{\Psi}^{(6)}), \tag{5.18}$$

Ψ being a 6×6 matrix and $\mathbf{E}$ a constant 6×1 vector. From (5.15) and (5.17) we readily obtain

$$\left.\begin{aligned}\begin{pmatrix} P_0\Psi(0) \\ Q_1\Psi(\ell)\end{pmatrix}\mathbf{E} &= 2\mathrm{i}\begin{pmatrix}\mathcal{K}_0 & 0\\ 0 & -\mathcal{K}_1\end{pmatrix}\begin{pmatrix}\mathbf{A}_0\\ \mathbf{A}_1\end{pmatrix},\\ \begin{pmatrix} Q_0\Psi(0) \\ P_1\Psi(\ell)\end{pmatrix}\mathbf{E} &= -2\mathrm{i}\begin{pmatrix}\mathcal{K}_0 & 0\\ 0 & -\mathcal{K}_1\end{pmatrix}\begin{pmatrix}\mathbf{B}_0\\ \mathbf{B}_1\end{pmatrix}.\end{aligned}\right\}$$

Eliminating $\mathbf{E}$ we find that

$$\begin{pmatrix}\mathbf{B}_0\\ \mathbf{B}_1\end{pmatrix} = \widehat{S}\begin{pmatrix}\mathbf{A}_0\\ \mathbf{A}_1\end{pmatrix}, \tag{5.19}$$

where $\widehat{S}$ is the extended 6×6 scattering matrix given by

$$\widehat{S} = -\begin{pmatrix}\mathcal{K}_0 & 0\\ 0 & -\mathcal{K}_1\end{pmatrix}^{-1}\begin{pmatrix} Q_0\Psi(0) \\ P_1\Psi(\ell)\end{pmatrix}\begin{pmatrix} P_0\Psi(0) \\ Q_1\Psi(\ell)\end{pmatrix}^{-1}\begin{pmatrix}\mathcal{K}_0 & 0\\ 0 & -\mathcal{K}_1\end{pmatrix},$$

which expresses the amplitudes of the scattered waves in terms of the incident wave amplitudes and $\Psi(\ell)$, $\Psi(0)$ being assigned. The most obvious way of choosing initial values for $\mathbf{\Psi}^{(i)}$ is to take $\Psi(0)=I$, the 6×6 identity matrix.

Denoting the elements of $\widehat{S}$ by $\widehat{S}_{ij}$ $(i,j=1,\ldots,6)$ and referring to the definition of the usual scattering matrix S in (5.6), we deduce from (5.19) that

$$S = \begin{pmatrix}\widehat{S}_{11} & \widehat{S}_{14}\\ \widehat{S}_{41} & \widehat{S}_{44}\end{pmatrix}.$$

An intrinsic property of S may be noted at this point. Referring to (5.7) we see that, because the governing equations are real-valued, $\overline{\phi}$ satisfies the same boundary value problem as ϕ except for the notational changes that $(\overline{B}_0,\overline{A}_0)^T$ replaces $(A_0,B_0)^T$ and $(\overline{B}_1,\overline{A}_1)^T$ replaces $(A_1,B_1)^T$. It follows from (5.6) that solving the problem for $\overline{\phi}$ will lead to

$$\begin{pmatrix}\overline{A}_0\\ \overline{A}_1\end{pmatrix} = S\begin{pmatrix}\overline{B}_0\\ \overline{B}_1\end{pmatrix}$$

and therefore, eliminating $(A_0,A_1)^T$ and $(B_0,B_1)^T$,

$$S\overline{S} = I.$$

This equation implies a set of relationships between the components of S identical to those derived by Kreisel (1949) for free surface motions. It applies to the exact solution of the boundary value problem posed in Section 2 and to the approximate solution, since (5.7) is common to both. As it is identically satisfied whatever $\Psi(x)$ may be, it is obviously not a check on a numerical solution method.

A computational check can be obtained, however, by deriving an energy equation for the approximate solution. It follows easily from (5.1) that

$$\Big[a(\overline{\phi}_0\phi_0' - \phi_0\overline{\phi}_0') - \kappa(\overline{\phi}_1\phi_2' - \phi_1\overline{\phi}_2' + \overline{\phi}_2\phi_1' - \phi_2\overline{\phi}_1')\Big]_{x_0}^{x_1} = 0. \tag{5.20}$$

The jump conditions show that quantity in brackets is continuous even where D' and H' are not (it is also continuous across cracks where D is discontinuous) and the equation therefore holds for any pair of points x_0 and x_1. In particular, letting $x_0\to-\infty$ and $x_1\to\infty$ and using (5.12) and (5.16), (5.20) gives

$$\left.\begin{aligned} E_0(|A_0|^2-|B_0|^2) + E_1(|A_1|^2-|B_1|^2) &= 0,\\ E_i = k_ia_i + 2\kappa^{-1}\beta_i k_i^5\tanh^2(k_iH_i).&\end{aligned}\right\} \tag{5.21}$$

This is also the wave energy balance for the unapproximated problem, which is not surprising as the approximate solution has the form of the exact solution for $|x| \to \infty$, as we noted after (5.7).

5.2. *Numerical results*

Numerical results have been obtained for the two-dimensional scattering problem described in section 5.1 for a variety of different geometrical configurations. The NAG routine, D02CJF which implements a variable-order, variable-step Adam's method, is used for the computation of $\Psi(x)$ over the varying part of the ice/bed.

There are no results in the literature against which the numerical results can be checked for accuracy. The energy balance relation given by (5.21), satisfied by both the full linear problem and the approximation, can be used as a check on the numerical scheme and consequently on the numerical solver described above. In all figures presented here, (5.21) was satisfied to at least four significant figures. The accuracy of the numerical solver breaks down when the wavelength in the ice (λ) is small compared with the length of the varying part of the bed. This is due to the growth of exponential solutions associated with the complex roots of the dispersion relation. A more sophisticated numerical method should therefore be implemented when results for smaller values of λ/l are considered.

In all of the results presented in this section we use the physical parameters for ice given by Squire *et al.* (1995). Thus, we take $E = 5\text{GPa}$, $\nu = 0.3$, $\rho_w = 1025\text{kgm}^{-3}$, $\rho_i = 922.5\text{kgm}^{-3}$, $g = 9.81\text{ms}^{-2}$. It is also known that ice sheets in the MIZ are usually between 0.5m and 2m thick, and we use this to guide our selection of $D(x)$. Finally, we choose the varying ice thickness so that each segment of the ice would be neutrally buoyant in the absence of surrounding ice, implying that $d(x) = (\rho_i/\rho_w)D(x)$ be satisfied. Of course, when there is total coverage of the fluid such a condition is unnecessary although it does ensure that there are no internal stresses within the ice when it is at rest.

In order to isolate the effects of wave reflection by ice of variable thickness and by the undulating topography, we consider the two cases separately. Thus, in the first examples, we take a flat bed and vary the thickness of the ice and, in particular, we consider the ice thickness given by the functions

$$D(x) = D_0 + \tfrac{1}{2}A_D(1 - \cos(2\pi x/l)), \tag{5.22}$$

$$D(x) = D_0 + 4A_D x(l-x)/l^2, \tag{5.23}$$

$$D(x) = D_0 + A_D x/l, \tag{5.24}$$

for $0 < x < l$. The first two represent local bulges in the ice of size $D_0 + A_D$, with $D_0 = D_1$, whilst the last represents a linear increase in ice thickness over the interval $(0, l)$ with $D_1 = D_0 + A_D$. In figures 1 and 2 the variation of reflection coefficient with dimensionless wavelength $\lambda/D_0 = 2\pi/(k_0 D_0)$. In these four figures, the transmission coefficient is obtained from $|T_0|^2 = 1 - |R_0|^2$ whilst $|R_1| = |R_0|$ and $|T_1| = |T_0|$. All figures confirm that total transmission occurs in the two limits as the wavelength tends to zero and infinity. In the first figure, 1(a), the four curves show the effect of the length of the varying part of the ice thickness on the reflection coefficient. For a longer section of varying ice thickness, the peak in the reflection coefficient decreases and occurs at longer wavelengths. In figure 1(b) we illustrate the effect that the size of the bulge in the ice, A_D, has on the reflection coefficient. As expected, the larger the bulge, the larger the value of $|R_0|$ over all wavelengths although increasing the value of A_D still further does not result in any occurrences of total reflection.

Figures 2(a) and (b) demonstrate the effects of varying the depth of the fluid and the

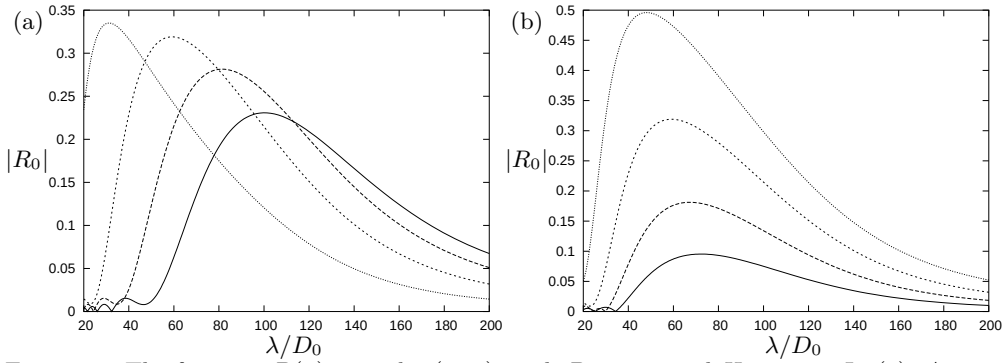

FIGURE 1. The function $D(x)$ given by (5.22), with $D_0 = 1$m and $H_0 = 20$m. In (a), $A_D = 1$m with $l = 80$m (solid), 60m (long dash), 40m (short dash) and 20m (dotted). In (b), $l = 40$m and $A_D = 0.25$m (solid), 0.5m (long dash), 1m (short dash), 2m (dotted).

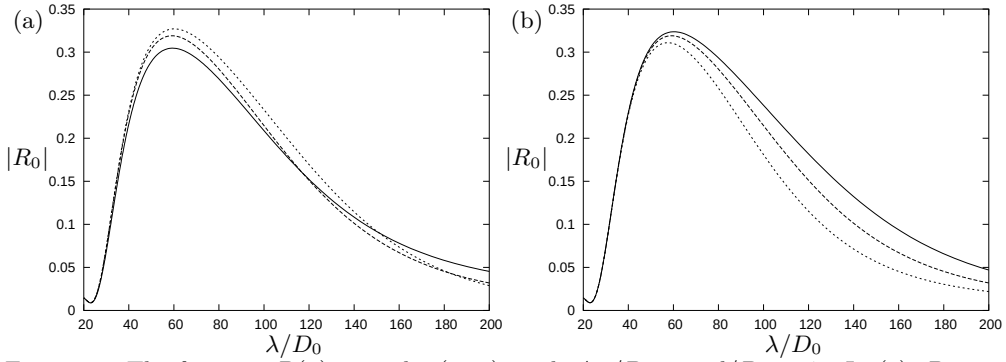

FIGURE 2. The function $D(x)$ given by (5.22), with $A_D/D_0 = 1$, $l/D_0 = 40$. In (a), $D_0 = 1$m with $H_0 = 40$m (solid), 20m (long dash), 10m (short dash). In (b), $H_0 = 20$m with $D_0 = 0.5$m (solid), 1m (long dash), 2m (short dash).

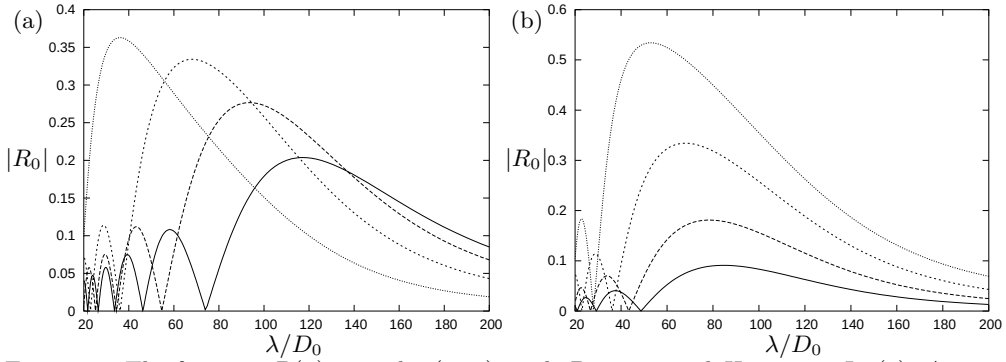

FIGURE 3. The function $D(x)$ given by (5.23), with $D_0 = 1$m and $H_0 = 20$m. In (a), $A_D = 1$m with $l = 80$m (solid), 60m (long dash), 40m (short dash) and 20m (dotted). In (b), $l = 40$m and $A_D = 0.25$m (solid), 0.5m (long dash), 1m (short dash), 2m (dotted).

thickness of the ice. In the former figure, depths of $H_0 = 10$m, 20m and 40m are used, whilst numerical experimentation shows that for depths greater than 40m, the reflection coefficient varies by less than 1% from those computed for $H_0 = 40$m over the range of wavelengths presented.

Figures 3(a), (b) are the counterparts of figures 1(a), (b) in the case of a parabolic

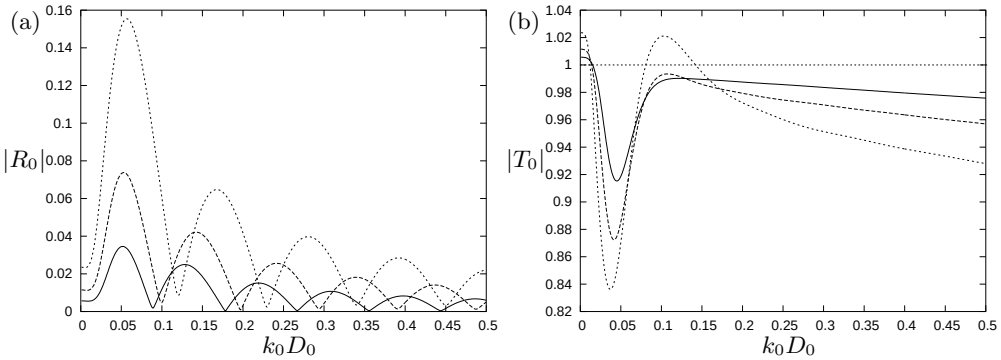

FIGURE 4. The function $D(x)$ given by (5.24), with $D_0 = 1$m, $H_0 = 20$m, $l = 40$m. In (a), $|R_0| = |R_1|$ and in (b), $|T_0|$ with $A_D = 0.5$m (solid), 1m (long dash), 2m (short dash).

ice profile given by (5.23). The principal difference is the presence of discontinuities in the $D'(x)$ at $x = 0$ and $x = l$, which appear to have a fairly significant effect on the reflection coefficient for smaller values of λ/D_0. For larger wavelengths, the behaviour of $|R|$ in figures 3(a), (b) is comparable with that shown in figures 1(a), (b). A similar phenomenon arises in free surface motions, where discontinuities in the bed slope can have a pronounced effect on wave reflection (see, for example, Porter (2003)).

Figure 4(a), (b) shows the variation of $|R_0|$ and $|T_0|$ with non-dimensional wavenumber k_0D_0 for the ice thickness profile given by (5.24). In this case, in which $D_0 \neq D_1$ and $H_0 \neq H_1$, $|R_1| = |R_0|$ whilst $|T_1| \neq |T_0|$ although a good approximation to $|T_1|$ is given by $1/|T_0|$. The periodic structure of R_0 is typical of problems in which there are two principal sources of wave reflection (in this case, the points $x = 0$ and $x = l$). Note that as $k_0D_0 \to 0$, the reflection coefficient tends to the shallow water limit given by Lamb (1932, §176), namely $|R_0| = (1 - \sqrt{H_1/H_0})/(1 + \sqrt{H_1/H_0})$, where in the three cases in figures 4(a) and (b), $H_1 = 19.55$m, 19.1m and 18.2m.

We now turn to the other aspect of this particular problem, which is to determine the effect of undulations in the bottom topography upon wave reflection, where the ice sheet has constant thickness. The two bed profiles that we focus on are given by the functions

$$H(x) = H_0 - \tfrac{1}{2}A_H(1 - \cos(2\pi x/l)), \tag{5.25}$$

$$H(x) = H_0 - A_H x/l, \tag{5.26}$$

for $0 < x < l$. The first represents a smoothly-varying local elevation in the topography of height A_H whilst the second represents a linear slope from the depth H_0 at $x = 0$ to $H_1 = H_0 - A_H$ at $x = l$. In the former case, we present in figures 5(a), (b) the variation of reflection coefficient with wavenumber for a selection of values of A_H and lengths l. As may be expected, the effect of increasing the size of the bed elevation is an increase in reflection and larger values of $|R_0|$ also result when the varying part of the bed is extended.

For the final example in this part of the paper, we consider the depth profile given by (5.26) and present the variation of $|R_0|$ and $|T_0|$ with k_0D_0 for a linear shoaling from $H_0 = 20$m to $H_1 = 10$m over the lengths, $l = 80$m to $l = 20$m. The corresponding results are shown in figure 6.

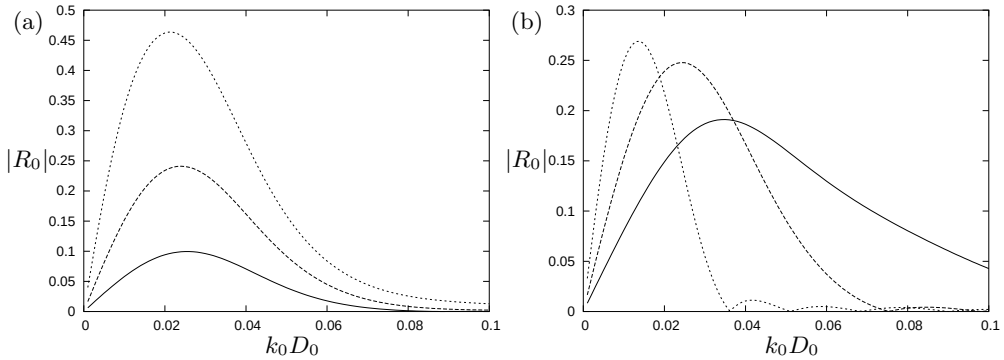

FIGURE 5. The function $H(x)$ given by (5.25), with $D_0 = 1$m, $H_0 = 20$m. In (a), $l = 80$m with $A_H = 5$m (solid), 10m (long dash), 15m (short dash) and in (b), $A_H = 10$m with $l = 40$m (solid), 80m (long dash), 160m (short dash).

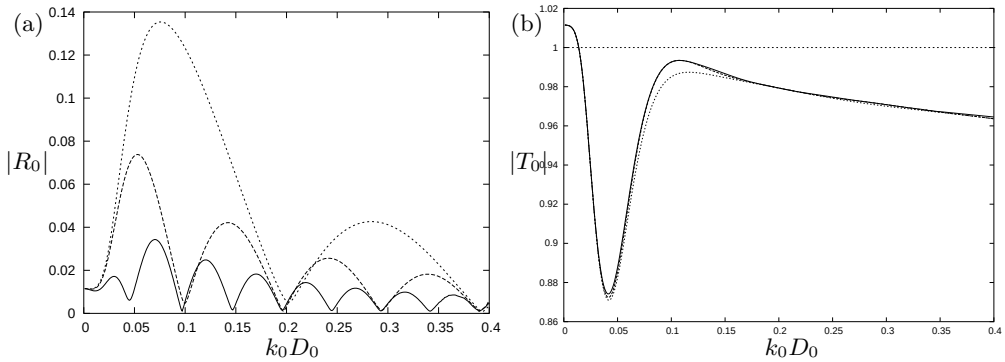

FIGURE 6. The function $H(x)$ given by (5.26), with $D_0 = 1$m, $H_0 = 20$m, $A_H = 10$m. In (a), $|R_0| = |R_1|$ and in (b) $|T_0|$ with $l = 40$m (solid), 20m (long dash), 10m (short dash).

6. Partial ice cover

We now address the more demanding problem in which the ice sheet occupies only a part of the whole surface. Our aim is to use the approximation developed in the previous sections in conjunction with the corresponding approximation for an unloaded free surface.

6.1. *The free surface case*

First we have to consider how the variational principle and its implementation are amended for $D = d = 0$. This is a straightforward matter of simplifying the existing expressions and it inevitably leads to the modified mild-slope equation derived by Chamberlain & Porter (1995). However, we need to give enough detail to establish the notation and to allow us to derive a unified approximation that encompasses both an ice sheet and a free surface.

Since $\alpha = \beta = 0$ in the reduced problem, the natural condition $\chi = [\psi]_0$ on $z = 0$ of the variational principle $\delta L_{\mathcal{D}} = 0$ is implied by (3.5) and this can be imposed as a constraint in $L_{\mathcal{D}}$ to give the functional

$$L_{\mathcal{D}}(\psi, [\psi]_0) \equiv L^{(0)}_{\mathcal{D}}(\psi) = \frac{1}{2}\iint_{\mathcal{D}} \Big\{ \int_{-h}^{0} (\nabla\psi)^2 \,\mathrm{d}z - \kappa[\psi]_0^2 \Big\} \,\mathrm{d}x\,\mathrm{d}y, \tag{6.1}$$

appropriate to free surface motions. We will use the superscript (0) to indicate that the quantities involved refer to the free surface case. The natural conditions of $\delta L^{(0)}_{\mathcal{D}} = 0$

with $\delta\psi = 0$ on $\mathcal{C} \times [-h, 0]$ may be deduced from (2.8) and (2.11) and they are

$$\nabla^2\phi = 0 \ (-h < z < 0), \quad \phi_z + \nabla_h h.\nabla_h\phi = 0 \ (z = -h), \quad \phi_z = \kappa\phi \ (z = 0), \tag{6.2}$$

the familiar free surface condition replacing (2.11). Only the element $\langle\langle\phi\rangle\rangle = 0$ of the jump conditions (3.7) is relevant in this case.

The reduced version of the approximation defined by (4.5) and (4.6) is

$$\left.\begin{array}{c} \phi(x,y,z) \approx \psi(x,y,z) = \varphi^{(0)}(x,y)w^{(0)}(x,y,z), \\ w^{(0)}(x,y,z) = \operatorname{sech}(k^{(0)}h)\cosh k^{(0)}(z+h), \\ k^{(0)}\tanh(k^{(0)}h) = \kappa, \end{array}\right\} \tag{6.3}$$

in which $k^{(0)}(h)$ denotes the positive real root of the truncated dispersion relation. We note that $k^{(0)}(h) = k(h, 0)$, where $k(H, D)$ is the positive real root of (4.6). An examination of the behaviour the roots $\pm k_0$, $\pm\mu_0$ and $\pm\overline{\mu}_0$ of (5.3) as $D_0 \to 0$ and $H_0 \to h_0$ shows that $|\mu_0| \to \infty$ and $k_0 \to k_0^{(0)}$, the solution of the reduced dispersion relation in (6.3) corresponding to $h = h_0$.

The result of setting $\psi = \varphi^{(0)}w^{(0)}$ in $\delta L_{\mathcal{D}}^{(0)} = 0$ can be deduced from (4.7), the second equation of which condenses to just $\chi = \varphi$. We may therefore eliminate χ and the system reduces to the single equation

$$\nabla_h.a^{(0)}\nabla_h\varphi^{(0)} + b^{(0)}\varphi^{(0)} = 0, \tag{6.4}$$

which is the modified mild-slope equation referred to earlier. The coefficients can be deduced from (4.12) and (4.13) and are

$$\left.\begin{array}{c} a^{(0)} = (4k^{(0)})^{-1}\operatorname{sech}^2(k^{(0)}h)\{2k^{(0)}h + \sinh(2k^{(0)}h)\}, \\ b^{(0)} = {k^{(0)}}^2 a^{(0)} - (W^{(0)}, W_h^{(0)})\nabla_h^2 h + C^{(0)}(\nabla_h h)^2, \\ C^{(0)} = (W^{(0)}, W_h^{(0)})_h - ||W_h^{(0)}||^2, \end{array}\right\}$$

where $W^{(0)}(x, y, z) = W(h, 0, z)$ in the notation of (4.12) and $H = h$ is implied in the definition of the inner product.

The jump condition satisfied by the solution of (6.4) where $\nabla_h h$ is discontinuous follows from (4.15) in the form

$$a^{(0)}\langle\mathbf{n}_\Gamma.\nabla_h\varphi^{(0)}\rangle + (W^{(0)}, W_h^{(0)})\langle\mathbf{n}_\Gamma.\nabla_h h\rangle\varphi^{(0)} = 0.$$

6.2. *The approximation*

We are now in a position to consider the problem of partial ice cover, in which (2.8) and (2.9) apply for a given domain $\mathcal{D}_i$ in the x, y plane and (6.2) applies for $\mathcal{D}_f$. As we have already derived approximations for the two components of this problem independently, the only outstanding issue is how the solutions of (4.7) and (6.4) have to be linked in the overall approximation.

To resolve this issue we require the secure framework of a composite variational principle that represents the hybrid case. This will obviously be based on the functionals $L_{\mathcal{D}}(\psi, \chi)$ defined in (3.3) and $L_{\mathcal{D}}^{(0)}(\psi)$ defined in (6.1). It is convenient to adapt notation that we used earlier and consider the domain $\mathcal{D} = \mathcal{D}_+ \cup \mathcal{D}_-$ in the x, y plane. We again denote by Γ the smooth curve where the two subdomains meet and use the subscripts $\pm$ to indicate the limiting values taken by functions on Γ or $\Gamma \times [-h, -d]$ from $\mathcal{D}_\pm$. Further, the unit vectors normal and tangential to Γ and the boundary coordinates introduced in Section 3.1 will be applied in the present context.

Suppose then that we remove the hypotheses that d and D be continuous and let an ice sheet with thickness $D > 0$ correspond to $\mathcal{D}_+$ and a free surface with $D = 0$ correspond to $\mathcal{D}_-$.

With the relevant elements of (3.4) in force, $\delta(L_{\mathcal{D}_+} + L^{(0)}_{\mathcal{D}_-}) = 0$ obviously implies the appropriate natural conditions (2.8) and (2.9) for $(x, y) \in \mathcal{D}_+$ and (6.2) for $(x, y) \in \mathcal{D}_-$. The contribution from the interface can be deduced from (3.6) as

$$\int_\Gamma \mathbf{n}.\Big\{\Big(\int_{-h}^{-d} \delta\psi\nabla_h\psi \,\mathrm{d}z\Big)_+ - \Big(\int_{-h}^{0} \delta\psi\nabla_h\psi \,\mathrm{d}z\Big)_- \\ +\{(\beta\nabla_h^2\chi)\nabla_h(\delta\chi) - \delta\chi\nabla_h(\beta\nabla_h^2\chi) - (1-\nu)\mathbf{c}\}_+\Big\} \,\mathrm{d}s.$$

We assume that χ_+ and $(\nabla_h\chi)_+$ are bounded and that $\psi_+ = \psi_-$ on $\Gamma\times[-h, -d]$, implying the coupling $\delta\psi_+ = \delta\psi_-$ there between the two functionals. The calculation leading to (3.7) applies with only the minor adjustment that one-sided edge conditions replace jump conditions and the natural conditions satisfied by the stationary point $\psi = \phi$, $\chi = \eta$ at the interface follow at once as

$$\mathbf{n}.\nabla_h\phi = 0 \quad ((x, y) \in \Gamma, -d \le z \le 0), \tag{6.5}$$

and

$$\langle\!\langle \mathbf{n}.\nabla_h\phi \rangle\!\rangle = (\mathcal{M}\eta)_+ = (\mathcal{S}\eta)_+ = 0. \tag{6.6}$$

Thus, finding the stationary point of $L_{\mathcal{D}_+} + L^{(0)}_{\mathcal{D}_-}$ is equivalent to satisfying the relevant equations, including the appropriate conditions at the interface that the bending moment and shear stress of the sheet must vanish at its edge and the normal fluid velocity must be zero on the edge of the sheet and continuous elsewhere. The continuity of pressure is imposed by the essential condition $\langle\!\langle\psi\rangle\!\rangle = 0$ which implies that ϕ is continuous on $\Gamma \times [-h, -d]$.

At this point we make the simplifying assumption that $d \to 0$ at the edge of the sheet, that is, $d_+ = 0$, but we retain the condition $D_+ > 0$. It is not significant that the approximation we are using cannot be made to satisfy (6.5) as that is a natural condition of the variational principle and not an essential condition. There is an issue at the interface, however, which we do have to address. Our existing trial functions defined by (4.5) and (6.3), namely,

$$\left.\begin{aligned} \psi(x, y, z) = \varphi(x, y)w(x, y, z) \quad ((x, y) \in \mathcal{D}_+, -h \le z \le -d), \\ \psi(x, y, z) = \varphi^{(0)}(x, y)w^{(0)}(x, y, z) \quad ((x, y) \in \mathcal{D}_-, -h \le z \le 0)), \end{aligned}\right\} \tag{6.7}$$

violate the essential condition $\psi_+ = \psi_-$ because $D_+ > 0$ implies that $w \ne w^{(0)}$. An apparently simple resolution of this difficulty is to abandon the hypothesis $D_+ > 0$ but we reject it on two grounds. First, it limits the generality of the model and second because the moduli of the four complex roots of the dispersion relation (4.6) tend to infinity as $D \to 0$, as we noted earlier, and this would give rise to computational difficulties in implementing the model. Therefore, in order to use the existing approximations and retain (4.7) and (6.4) we instead remove the essential condition that leads to the conflict and modify the variational principle so that $\langle\!\langle\phi\rangle\!\rangle = 0$ is a natural condition.

This is achieved by introducing the auxiliary variable $u(x, y, z)$ $((x, y) \in \Gamma, -h \le z \le 0)$ as a Lagrange multiplier and the functional

$$I(\psi_+, \psi_-, u) = \int_\Gamma \int_{-h}^{0} (\psi_+ - \psi_-)u \,\mathrm{d}z \,\mathrm{d}s,$$

which takes account of the simplification that $d = 0$ at the interface. Then the contribution to $\delta(L_{\mathcal{D}_+} + L^{(0)}_{\mathcal{D}_-} - I)$ on Γ involving $\psi_\pm$ is

$$\widetilde{C}_\Gamma \equiv \int_\Gamma \int_{-h}^0 \Big\{ \delta\psi_+ \{\mathbf{n}.(\nabla_h \psi)_+ - u\} - \delta\psi_- \{\mathbf{n}.(\nabla_h\psi)_- - u\} - (\psi_+ - \psi_-)\delta u \Big\} \, \mathrm{d}z \, \mathrm{d}s. \quad (6.8)$$

As $\widetilde{C}_\Gamma$ must vanish for arbitrary variations $\delta\psi_\pm$ and δu it follows that the stationary point $\psi = \phi$ of the extended functional does indeed satisfy the natural jump condition $\langle\!\langle \phi \rangle\!\rangle = 0$, in addition to those given in (6.6), and that $u = \mathbf{n}.(\nabla_h\phi)_+ = \mathbf{n}.(\nabla_h\phi)_-$ at the stationary point. The coupling between the functionals defined on $\mathcal{D}_\pm$ is provided by I in the revised principle, which does not require ψ to be continuous across $\Gamma \times [-h, 0]$. Therefore the natural conditions, including $\langle\!\langle \phi \rangle\!\rangle = 0$, can be satisfied arbitrarily closely by choosing the basis for the approximation $\psi \approx \phi$ to be large enough. One possibility is to extend (6.7) to include the eigenfunctions corresponding to evanescent modes, as has been implemented in the case of the mild-slope equation by Porter & Staziker (1995) and Athanassoulis & Belibassakis (1999).

The present purpose is to use (6.7) as it stands, expressed for convenience in the form $\psi(x, y, z) = \varphi(x, y)w(x, y, z)$ for $(x, y) \in \mathcal{D}\backslash\Gamma$, with the superscripts temporarily suppressed for $(x, y) \in \mathcal{D}_-$. A approximation that is of the same order as (6.7) and consistent with it, in the sense of allowing the variable z to be integrated out, is also required for u and we therefore take $u(x, y, z) = \tilde{u}(x, y)v(x, y, z)$, in which v is assumed to be known. It follows by substituting the approximations into (6.8) that $\widetilde{C}_\Gamma$ vanishes for arbitrary variations $\delta\varphi_\pm$ and $\delta\tilde{u}$ provided that

$$\int_{-h}^0 w_\pm \{\mathbf{n}.(\nabla_h(\varphi w))_\pm - \tilde{u}\, v\} \, \mathrm{d}z = 0, \quad \int_{-h}^0 \{\varphi_+ w_+ - \varphi_- w_-\}\, v \, \mathrm{d}z = 0. \quad (6.9)$$

The final equation may be recognised as a weak form of $\langle\!\langle \psi \rangle\!\rangle = 0$ and all three may be combined to give

$$\Big\langle \int_{-h}^0 (\varphi w)\, \mathbf{n}.\nabla_h(\varphi w) \, \mathrm{d}z \Big\rangle = 0,$$

which represents conservation of depth-averaged energy flux across Γ.

The basis function v approximates the vertical structure of the normal velocity across the interface between the two fluid regions. We therefore represent it in terms of w_+ and w_- by taking $v = c_+ w_+ + c_- w_-$ and ensure that it has the same average with respect to both. Thus we choose $c_\pm$ so that $(w_+, v) = (w_-, v)$, in which the inner product used earlier applies with $H = h$. With this choice and elimination of $\tilde{u}$, (6.9) implies the jump conditions

$$\Big\langle \int_{-h}^0 w\, \mathbf{n}.\nabla_h(\varphi w) \, \mathrm{d}z \Big\rangle = 0, \quad \langle\varphi\rangle = 0. \quad (6.10)$$

(It can be shown that constants $c_\pm$ exist so that v has the required properties, but their values are not required.)

We are now in a position to give the full set of natural conditions that results from using (6.7) with the variational principle $\delta\{L_{\mathcal{D}_+} + L^{(0)}_{\mathcal{D}_-} - I\} = 0$. It consists of (4.7), holding for $(x, y) \in \mathcal{D}_+$, (6.4), holding for $(x, y) \in \mathcal{D}_-$, and the jump conditions

$$\left.\begin{aligned} \varphi - \varphi^{(0)} = (\mathcal{M}\chi)_+ = (\mathcal{S}\chi)_+ = 0, \\ a\mathbf{n}.\nabla_h\varphi + \varphi\mathbf{n}.\{(W, W_H)\nabla_h H + (W, W_D)\nabla_h D\}_+ = \\ a^{(0)}\mathbf{n}.\nabla_h\varphi^{(0)} + \varphi^{(0)}\mathbf{n}.\{(W^{(0)}, W^{(0)}_h)\nabla_h h\}_-, \end{aligned}\right\} \quad (6.11)$$

holding on Γ. These incorporate (6.10) with the notation of (6.7) restored and the transformation (4.12) from w to W carried out.

6.3. *A two-dimensional problem*

We return to the two-dimensional setting to illustrate how the solution of the equations governing partial ice cover may be implemented.

There is considerable scope for combining a variable bedform and an ice sheet of finite or semi-infinite extent. We consider here the simple example in which the ice sheet occupies the interval $0 \le x \le \ell$ and take the mean water depth to be constant for $x < 0$ and $x > \ell$. It is convenient to adopt the notation of section 4.1 as far as possible and we set

$$\left.\begin{aligned} h(x) &= h_0, \quad (x < 0), \\ h(x) &= h_1, \quad (x > \ell). \end{aligned}\right\}$$

It is assumed that the sheet elevation and thickness satisfy $d(0+) = d(\ell-) = 0$, $D(0+) > 0$ and $D(\ell-) > 0$, consistent with the theory developed above. We also suppose that $h'(x)$, $d'(x)$ and $D'(x)$ are continuous for $0 < x < \ell$.

Within the semi-infinite regions, the solutions of (6.4) may be taken in the forms

$$\varphi^{(0)} = \left\{ \begin{array}{ll} A_0 \mathrm{e}^{\mathrm{i}k_0^{(0)}x} + B_0 \mathrm{e}^{-\mathrm{i}k_0^{(0)}x} & (x < 0), \\ A_1 \mathrm{e}^{\mathrm{i}k_1^{(0)}(\ell - x)} + B_1 \mathrm{e}^{-\mathrm{i}k_1^{(0)}(\ell - x)} & (x > \ell), \end{array} \right\} \tag{6.12}$$

in which the wavenumber $k_i^{(0)}$ is that corresponding to the dispersion relation in (6.3) with $h = h_i$. As in the earlier example, the amplitudes of the scattered waves are determined through (5.6).

For $0 < x < \ell$, we use the form (5.1) of the equations and in terms of the variables occurring there, the jump conditions (6.11) to be applied at $x = 0$ are

$$\left.\begin{aligned} \phi_0(0+) = \varphi^{(0)}(0-), \quad \phi_2(0+) = \phi_2'(0+) = 0, \\ a_0\phi_0'(0+) + j(0+)\phi_0(0+) = a_0^{(0)}\varphi^{(0)\,\prime}(0-), \end{aligned}\right\} \tag{6.13}$$

since $h'(0-) = 0$. Here we have introduced the jump coefficient

$$j(0+) = (W, W_H)_0 H'(0+) + (W, W_D)_0 D'(0+)$$

and used the subscripts 0 and 1 to indicate that a term is to be evaluated at $H = h = h_0$ and $H = h = h_1$, respectively.

The corresponding conditions prevailing at $x = \ell$ are

$$\left.\begin{aligned} \phi_0(\ell-) = \varphi^{(0)}(\ell+), \quad \phi_2(\ell-) = \phi_2'(\ell-) = 0, \\ a_1\phi_0'(\ell-) + j(\ell-)\phi_0(\ell-) = a_1^{(0)}\varphi^{(0)\,\prime}(\ell+), \end{aligned}\right\} \tag{6.14}$$

where

$$j(\ell-) = (W, W_H)_1 H'(\ell-) + (W, W_D)_1 D'(\ell-).$$

The system (5.8) has to be solved again, subject to appropriate boundary conditions. By combining (6.12), (6.13) and (6.14) we find that

$$\begin{aligned} F_0 \begin{pmatrix} \boldsymbol{\Phi}(0+) \\ U_0\boldsymbol{\Phi}'(0+) \end{pmatrix} = 2\mathrm{i}k_0^{(0)}a_0^{(0)}\mathbf{A}_0, \quad \overline{F}_0 \begin{pmatrix} \boldsymbol{\Phi}(0+) \\ U_0\boldsymbol{\Phi}'(0+) \end{pmatrix} = -2\mathrm{i}k_0^{(0)}a_0^{(0)}\mathbf{B}_0, \\ \overline{F}_1 \begin{pmatrix} \boldsymbol{\Phi}(\ell-) \\ U_1\boldsymbol{\Phi}'(\ell-) \end{pmatrix} = -2\mathrm{i}k_1^{(0)}a_1^{(0)}\mathbf{A}_1, \quad F_1 \begin{pmatrix} \boldsymbol{\Phi}(\ell-) \\ U_1\boldsymbol{\Phi}'(\ell-) \end{pmatrix} = 2\mathrm{i}k_1^{(0)}a_1^{(0)}\mathbf{B}_1, \end{aligned} \tag{6.15}$$

where U is defined by (5.9), $\mathbf{A}_i = (A_i, 0, 0)^T$, $\mathbf{B}_i = (B_i, 0, 0)^T$, and F_i is the 3×6 matrix given by

$$F_i = \begin{pmatrix} f_i & 0 & 0 & 1 & 0 & 0 \\ 0 & 0 & 1 & 0 & 0 & 0 \\ 0 & 0 & 0 & 0 & 0 & 1 \end{pmatrix}$$

with

$$f_0 = j(0+) + \mathrm{i}k_0^{(0)}a_0^{(0)}, \quad f_1 = j(\ell-) + \mathrm{i}k_1^{(0)}a_1^{(0)}.$$

Applying (6.15) to the solution for $0 < x < \ell$ in the form (5.18) easily leads to the scattering matrix in the form

$$S = -\begin{pmatrix} k_0^{(0)}a_0^{(0)} & 0 \\ 0 & -k_1^{(0)}a_1^{(0)} \end{pmatrix}^{-1} \begin{pmatrix} G_{11} & G_{14} \\ G_{41} & G_{44} \end{pmatrix} \begin{pmatrix} k_0^{(0)}a_0^{(0)} & 0 \\ 0 & -k_1^{(0)}a_1^{(0)} \end{pmatrix},$$

where

$$G = \begin{pmatrix} \overline{F}_0\boldsymbol{\Psi}(0) \\ F_1\boldsymbol{\Psi}(\ell) \end{pmatrix} \begin{pmatrix} F_0\boldsymbol{\Psi}(0) \\ \overline{F}_1\boldsymbol{\Psi}(\ell) \end{pmatrix}^{-1}.$$

The identity $S\overline{S} = I$ holds as in Section 5, and so does (5.20) with $x_0 = 0+$ and $x_1 = \ell-$. The scalar counterpart of (5.20) applying in the free surface regions is

$$\left[a^{(0)}(\overline{\varphi}^{(0)}\varphi^{(0)\prime} - \varphi^{(0)}\overline{\varphi}^{(0)\prime})\right]_{x_0}^{x_1} = 0,$$

where $x_0 < x_1 < 0-$ or $\ell+ < x_0 < x_1$. We can combine two versions of this equation with (5.20) so as to encompass the whole interval $-\infty < x < \infty$. By using (6.13) and (6.14) at the junctions and (6.12) to evaluate the contributions as $|x| \to \infty$, we readily find that

$$k_0^{(0)}a_0^{(0)}(|A_0|^2 - |B_0|^2) + k_1^{(0)}a_1^{(0)}(|A_1|^2 - |B_1|^2) = 0. \tag{6.16}$$

This equation is also satisfied by the far-field wave amplitudes in the exact solution. It can be deduced directly from (5.21) by setting $\beta_0 = \beta_1 = 0$ there.

6.4. *Numerical results*

The first task is to establish the accuracy of the model that we have presented in this new setting. We remark that we do not expect the results in the case of partial ice cover to be as accurate as those in the case where there is total ice cover. This is because there is now an extra source of scattering not present previously, namely at the ends of the ice sheet. Although the variational principle has been adapted in order to satisfy continuity of pressure and mass flux, it is recognised that the one term approximations used may struggle to resolve the scattering process at the interface between the ice-covered and free surface regions.

As in Section 5.2, where the case of total ice cover is considered, the energy balance equations, given for the present case by (6.16), can be used as a check on the accuracy of the numerical solver, and comments similar to those described in Section 5.2 also apply here.

Further evidence of the accuracy of the method can be obtained by referring to established results.

Many authors who have considered the effect on waves of a thin, finite elastic sheet floating on water have chosen to focus on the elevation of the sheet rather than the reflection and transmission coefficients. Those that have produced results for the scattering coefficients (Andrianov & Hermans (2003) and Tkacheva (2002)) provide insufficient details of the parameters that they used to allow comparison with our results. In contrast,

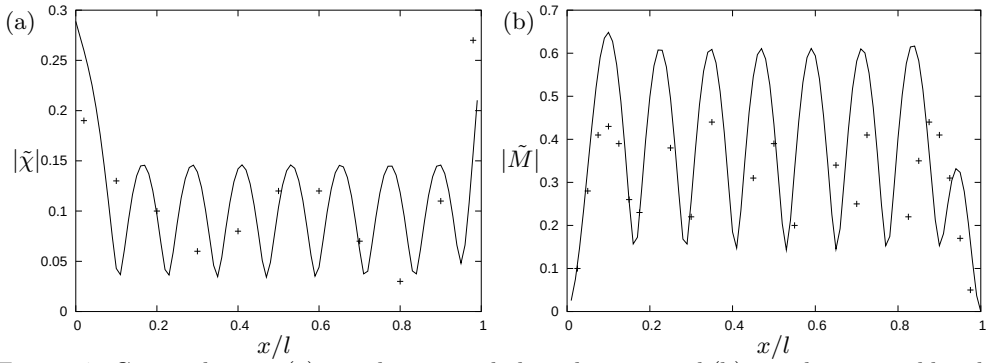

FIGURE 7. Curves showing (a) non-dimensional plate elevation and (b) non-dimensional bending moment against length of plate for an incident wave period of $\tau = 0.7$s. The dots show the experimental results of Utsunomiya *et al.* (1995).

Wu *et al.* (1995) list a detailed set of parameters in their analysis of wave interaction with a finite length floating platform of constant thickness, in which they compared theoretical results for sheet elevation and bending moments with the experimental results of Utsunomiya *et al.* (1995).

In Wu *et al.* (1995), $E = 103$MPa, $\nu = 0.3$, $\rho_i = 220.5$kgm^3, $l = 10$m, $D(x) = D_0 = 38$mm, and $H_0 = 1.1$m. The draught of their sheet is 8.4mm, but we have set this to zero for our calculations as we have restricted ourselves to the case where $d(x) \to 0$ as $x \to 0, l$. A similar assumption was made by Tkacheva (2002) who also compared results for bending moments along the sheet to those given in Wu *et al.* (1995). The incident wave has a period of $\tau = 0.7$s in figure 7 and $\tau = 1.429$s in figure 8. Each figure shows the variation along the plate of non-dimensional sheet elevation, $|\tilde{\chi}| = |\chi(x)/A_0|$, and bending moment, $|\tilde{M}| = (\rho_w D_0/l\rho_i)\phi_2(x)$. The functions $\chi(x) = \phi_1(x)$ and $\phi_2(x)$ are easily obtained from $\Psi(x)$, whilst other quantities such as the dynamic pressure under the sheet and the shearing stress are proportional to $\phi_0(x)$ and $\phi_2'(x)$ and are therefore also readily obtained.

Despite the cautionary remark about accuracy made above, the results we have obtained are in good agreement with those of Wu *et al.* (1995), Tkacheva (2002) and Khabakhpasheva & Korobkin (2002), having the correct behaviour, although there are slight discrepancies in the size of the elevation at the ends of the plate. The experimental results of Utsunomiya *et al.* (1995) are overlaid onto the figures for comparison.

It is worth noting that in this numerical experiment, where the sheet is of constant thickness, there is, of course, an analytic solution for $\Psi(x)$ composed of the set (5.11), namely,

$$\Psi(x) = \begin{pmatrix} C_0 g(x) & C_0\overline{g(x)} \\ \mathrm{i}U_0 C_0 \mathcal{K}_0 g(x) & -\mathrm{i}U_0 C_0 \mathcal{K}_0 \overline{g(x)} \end{pmatrix}, \quad g(x) = \mathrm{diag}(\mathrm{e}^{\mathrm{i}k_0 x}, \mathrm{e}^{\mathrm{i}\mu_0 x}, \mathrm{e}^{-\mathrm{i}\overline{\mu}_0 x}).$$

This analytic form for the solution over the ice has been used as a check on the numerical solver.

In the example considered above we made the assumption that $d(x) = 0$ for $0 < x < l$ in order to compare with existing work. We now consider examples in which we require only that $d(x) \to 0$ as $x \to 0, l$ whilst Archimede's principle is imposed to ensure that the ice sheet is neutrally buoyant. That is, we require that the integral of $\rho_i D(x) - \rho_w d(x)$ over $0 < x < l$ to be zero. Let us consider an ice sheet having a horizontal upper surface

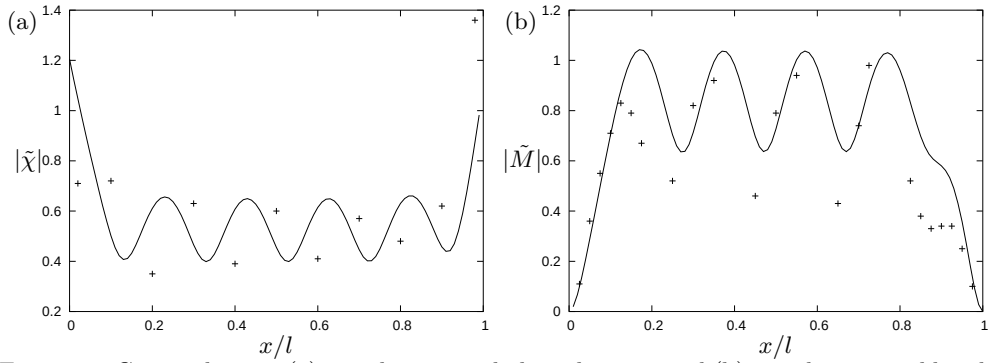

FIGURE 8. Curves showing (a) non-dimensional plate elevation and (b) non-dimensional bending moment against length of plate for an incident wave period of $\tau = 1.429$s. The dots show the experimental results of Utsunomiya *et al.* (1995).

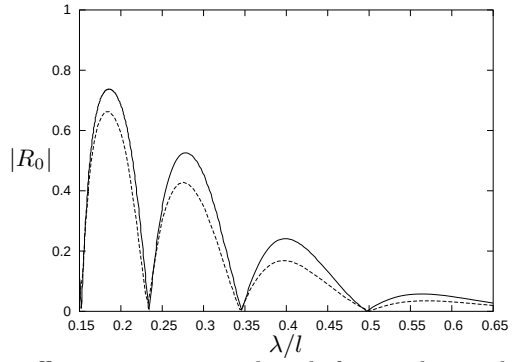

FIGURE 9. Reflection coefficient against wavelength for an elastic plate of constant thickness $D_0 = 38$mm (solid) and one with the parabolic profile given by (6.20) with $D_0 = 30$mm (dashed).

and a parabolic lower surface such that

$$D(x) = D_0 + 4A_D(1 - x/l)(x/l), \tag{6.17}$$

where $D_0 + A_D$ is the maximum thickness of the sheet. Then $d(x) = -4A_D(1-x/l)(x/l)$ and Archimedes principle implies that $A_D = \frac{3}{2}\rho_i D_0/(\rho_w - \rho_i)$. In the particular case considered previously, $\rho_i \approx \frac{1}{5}\rho_w$ and hence $A_D \approx \frac{3}{8}D_0$. Then, the 'average' thickness of the sheet described by (6.17) is $\frac{5}{4}D_0$. Hence, choosing a thickness profile in (6.17) with $D_0 = 30$mm will allow comparison with a sheet of constant thickness $D_0 = 38$mm considered previously.

The reflection coefficients for these two cases are plotted in figure 9 against the dimensionless wavelength λ/l (where now $\lambda = 2\pi/k_0^{(0)}$), and they show similar behaviour with slightly reduced reflection for the sheet with a parabolic profile compared with that of constant thickness. In figure 9 the wave period varies from $\tau = 0.98$s when $\lambda/l = 0.15$ to $\tau = 2.3$s when $\lambda/l = 0.65$.

For the remaining results, we revert to our original set of parameters for ice described in Section 5.2. As in the previous example, we use (6.17) to define the variation of ice thickess but now $A_D = 13.5D_0$, implying that the thickest part of the ice is 14.5 times the thickness at the edge of the ice. In figure 10 we have considered the effect of the length of the ice sheet on the reflection coefficient where $H_0 = 20$m and $D_0 = 0.1$m over a range of wavenumbers $k_0^{(0)}$.

Thus it can be seen that increasing the length of an ice sheet with the same maximum

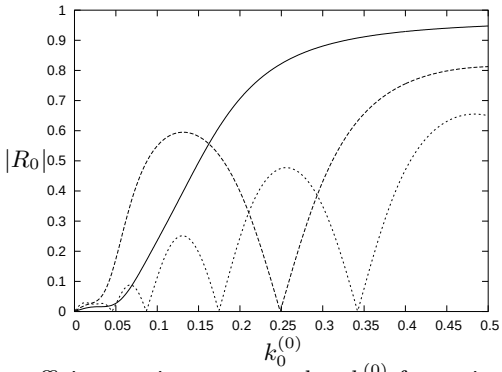

FIGURE 10. Reflection coefficient against wavenumber $k_0^{(0)}$ for an ice sheet with the parabolic profile given by (6.20) with $D_0 = 0.1$m, $H_0 = 20$m and $l = 40$m (solid), 80m (long dash) and 160m (short dash).

thickness reduces the amount of reflection as might be expected as the gradient of the thickness is reduced.

7. Conclusions

One of the main features of the work described here is the derivation of a variational principle that is equivalent to the linearised equations governing the motion of an elastic sheet of varying thickness and infinite or finite extent, floating on water of varying depth. The natural conditions of the principle include the edge conditions for a sheet of non-constant thickness, in addition to the field equation and the boundary conditions. The variational formulation can be used in conjunction with the Rayleigh-Ritz method to produce solutions for a range of full linear problems incorporated in the general setting, to any desired accuracy, and it is applicable to other situations which involve wave propagation in and by floating elastic sheets.

Here we have exploited the formulation in a particular way, using it to simplify the model and thereby obtain approximations at a significantly reduced computational cost. This has been achieved by replacing the vertical component of the fluid motion locally by the eigenfunction that supports propagating waves for an ice sheet of constant thickness on water of constant depth. The approach therefore extends to the problem under consideration the "mild-slope approximation" used previously for purely free surface motions. This procedure is itself an extension of shallow water theory to the general wavelength régime.

The accuracy of the approximation can only be ascertained by comparing numerical results for the model with the "exact" solutions of test problems. As suggested above, the latter could be obtained by returning to the variational principle and taking an N-dimensional basis for the approximation by including the vertical eigenfunctions corresponding to $N-1$ evanescent modes. Numerical experiments will determine the value of N required to achieve a given convergence criterion. This process has been carried out for the mild-slope approximation to free surface flows by Porter & Staziker (1995) and Athanassoulis & Belibassakis (1999), the latter authors obtaining superior convergence by extending the basis in a particular way. This and other evidence in the form of comparisons with experimental data and with full linear solutions obtained by other means, including that for periodic beds given recently by Porter & Porter (2003), indicates that the mild-slope approach provides a good approximation for free surface motions, as long

as the bedform gradient is not too large. On this basis, we suppose that the one-term trial function used in the present problem is also likely to lead to a reasonable first approximation, at least for moderate bedform and ice thickness slopes.

In addition to the multi-mode exploitation of the variational principle, the generality of the formulation allows a wide range of problems to be considered using just the single mode approximation. Here we have restricted attention to particular examples of two-dimensional scattering, to show how numerical solutions can be constructed and demonstrate the overall viability of the approach. The model equations derived can be applied directly to three dimensional problems, such as wave scattering by a circular ice sheet, wave trapping and crack problems (similar to those consider by Khabakhpasheva & Korobkin (2002) for example), and the interplay between and individual effects of ice sheet thickness and depth variations can be explored more thoroughly than we have attempted here.

Appendix

We require the values of the various inner products involving $W(H, D, Z)$ and its derivatives that occur in (4.13), where W is given in (4.12). The wavenumber $k(H, D)$ occurring in W is defined implicitly by (4.6), which can be expressed in the form

$$f(k, D)\tanh(kH) = \kappa, \quad f(k, D) = \{1 - \alpha(D) + \beta(D)k^4\}k. \tag{A1}$$

Now

$$W_H = k_H\ \mathrm{sech}(kH)Z\sinh k(Z + H) + (kH)_H\ \mathrm{sech}^2(kH)\sinh(kZ),$$
$$W_D = k_D\{\mathrm{sech}(kH)Z\sinh k(Z + H) + H\mathrm{sech}^2(kH)\sinh(kZ)\},$$

and it follows by direct integration that

$$2(W, W_H) = (k_H/4k^2)\ \mathrm{sech}^2K\{2K - \sinh(2K) - 4K^2\tanh K\}$$
$$-K\mathrm{sech}^2K\tanh K,$$
$$2(W, W_D) = (k_D/4k^2)\ \mathrm{sech}^2K\{2K - \sinh(2K) - 4K^2\tanh K\},$$

in which the abbreviation $K = kH$ has been used.

We note that the identity $(W, W_H)_H - ||W_H||^2 = (W, W_{HH}) + (WW_H)_{Z=-H}$ gives an alternative way of calculating the value of this term and similarly for the other coefficients of the same form. Referring to the notation (4.14) we find that

$$C^{(1)} = \mathrm{sech}^2K\{(k_{HH}/8k^2)A + (k_H^2/8k^3)B + (k_H/2k)C$$
$$+k\tanh K(K\tanh K - 1)\},$$
$$C^{(2)} = \mathrm{sech}^2K\{(k_{DD}/8k^2)A + (k_D^2/8k^3)B\},$$
$$C^{(3)} = \mathrm{sech}^2K\{(k_{HD}/4k^2)A + (k_Hk_D/4k^3)B + (k_D/2k)C\},$$

in which

$$A = 2K - \sinh(2K) - 4K^2\tanh K,$$
$$B = 8K^3\tanh^2 K - 4K^2\tanh K + \sinh(2K) - (8/3)K^3 - 2K,$$
$$C = 4K^2\tanh^2 K - K^2 - 5K\tanh K.$$

The required derivatives of k are readily found from (A1) and are given by

$$Ek_H = -2fk, \quad Ek_D = -f_D \sinh(2K),$$

$$Ek_{HH} = -Fk_H^2 - 4k_H\{f + kf_k \cosh^2 K\},$$

$$Ek_{DD} = -Fk_D^2 - 2k_D\{f_{kD} \sinh(2K) + 2Hf_D \cosh^2 K\} - f_{DD} \sinh(2K),$$

$$Ek_{HD} = -Fk_Hk_D - k_H\{f_{kD} \sinh(2K) + 2Hf_D\} - 2k_D\{f + kf_k\} - 2kf_D,$$

in which

$$E = f_k \sinh(2K) + 2Hf, \quad F = f_{kk} \sinh(2K) + 4Hf_k \cosh^2 K.$$

The derivatives of f are

$$f_k = 1 - \alpha + 5\beta k^4, \quad f_D = -D^{-1}k(\alpha - 3\beta k^4),$$

$$f_{kk} = 20\beta k^3, \quad f_{kD} = -D^{-1}(\alpha - 15\beta k^4), \quad f_{DD} = 6D^{-2}\beta k^5,$$

in which the expressions for α and β given in (2.10) have been used.

In the case $d = D = 0$, (A1) reduces to the dispersion relation for an unloaded free surface with $f = k$. We then have

$$Ek_H = -2k^2, \quad E = 2K + \sinh(2K),$$

$$Ek_{HH} = -4Hk_H^2 \cosh^2 K - 4kk_H(1 + \cosh^2 K).$$

Using these equations and noting that $H = h$, it can be confirmed that the above expressions for the coefficients (W, W_H) and $C^{(1)}$ reduce to the corresponding terms given by Chamberlain & Porter (1995) for the modified mild-slope equation.

REFERENCES

Andrianov, A. I. & Hermans, A. J. 2003 The influence of water depth on the hydroelastic response of a very large floating platform. *Marine Structures* **16**, 355–371.

Athanassoulis, G. A. & Belibassakis, K. A. 1999 A consistent coupled-mode theory for the propagation of small-amplitude water waves over variable bathymetry regions. *J. Fluid Mech.* **389**, 275–301.

Balmforth, N. J. & Craster, R. V. 1999 Ocean waves and ice sheets. *J. Fluid Mech.* **395**, 89–124.

Berkhoff, J. C. W. 1973 Computation of combined refraction-diffraction. *Proc. 13th Conf. on Coastal Engng., July 1972, Vancouver, Canada*, vol. 2, pp. 471–490. ASCE.

Berkhoff, J. C. W. 1976 Mathematical models for simple harmonic linear waves. Wave diffraction and refraction. *Delft Hydr. Rep.* W 154-IV.

Chamberlain, P. G. & Porter, D. 1995 The modified mild-slope equation. *J. Fluid Mech.* **291**, 393–407.

Evans, D. V. & Davies, T. V., 1968 Wave-ice interaction. *Report No. 1313, Davidson Lab – Stevens Institute of Technology, New Jersey.*

Hermans, A. J. 2003a Interaction of free-surface waves with a floating dock. *J. Eng. Maths.* **45**, 39–53.

Hermans, A. J. 2003b The ray method for the deflection of a floating flexible platform in short waves. *J. Fluids Structures* **17**, 593–602.

Hermans, A. J. 2003c Interaction of free-surface waves with floating flexible strips. *(Preprint).*

Khabakhpasheva, T. I. & Korobkin, A. A. 2002 Hydroelastic behaviour of compund floating plate in waves *J. Eng. Maths.* **44**, 21–40.

Kashiwagi, M. 1998 A B-Spline Galerkin scheme for calculating hydroelastic response of a very large floating structure in waves. *J. Marine Sci. and Tech.* **3**, 37–49.

Kreisel, G. 1949 Surface waves. *Q. Appl. Maths* **7**, 21–44.

Lamb, H. 1932 Hydrodynamics. Cambridge University Press.

Linton, C. M. & Chung, H. 2003 Ocean waves and ice sheets. *Wave Motion* **38**, 43–52.

Meylan, M. H. 2001 A variational equation for the wave forcing of floating thin plates. *Appl. Ocean Res.* **23**, 195–206.

Meylan, M. H. & Squire, V. A. 1994 Response of ice floes to ocean waves. *J. Geophys. Res.* **99**, 891–905.

Meylan, M. H. & Squire, V. A. 1996 Response of a circular ice floe to ocean waves. *J. Geophys. Res.* **101**, 8869–8894.

Newman, J. N. 1994 Wave effects on deformable bodies. *Appl. Ocean Res.* **16**, 47–59.

Porter, D. 2003 The mild-slope equations. *J. Fluid Mech.* **494**, 51–63.

Porter, R. & Porter, D. 2003 Scattered and free waves over periodic beds. *J. Fluid Mech.* **483**, 129–163.

Porter, D. & Staziker, D. J. 1995 Extensions of the mild-slope equation. *J. Fluid Mech.* **300**, 367–382.

Smith, R. & Sprinks, T. 1975 Scattering of surface waves by a conical island. *J. Fluid Mech.* **72**, 373–384.

Squire, V. A. & Dixon, T. W. 2001 On modelling an iceberg embedded in shore-fast sea ice. *J. Eng. Math.* **40**, 211–226.

Squire, V. A., Dugan, J. P., Wadhams, P., Rottier, P. J., & Liu, A. K. 1995 Of ocean waves and ice sheets. *Ann. Rev. Fluid Mech.* **27**, 115–168.

Sturova, I. 2001 The diffraction of surface waves by an elastic platform floating on shallow water. *J. Appl. Maths. Mechs.* **65**(1), 109–117.

Takagi, K., Shimada, K. & Ikebuchi, T. 2000 An anti-motion device for a very large floating structure. *Marine Structures* **13**, 421–436.

Takagi, K. 2002 Surface wave diffraction on a floating elastic plate. *Appl. Ocean Res.* **24**, 175–183.

Timoshenko, S. & Woinowsky-Krieger, S. 1959 Theory of Plates and Shells, 2nd Edition. *McGraw-Hill, New York*.

Tkacheva, L. A. 2001a Scattering of surface waves by the edge of a floating elastic plate. *J. Appl. Mech. Tech. Phys.* **42**, 638–646.

Tkacheva, L. A. 2001b Hydroelastic behavior of a floating plate in water. *J. Appl. Mech. Tech. Phys.* **42**, 991–996.

Tkacheva, L. A. 2001c Surface wave diffraction on a floating elastic plate. *Fluid Dynamics* **36**, 776–789.

Tkacheva, L. A. 2002 Diffraction of surface waves at a thin elastic floating plate. *Proc. 17th Int. Workshop on Water Waves and Floating Bodies, Cambridge, UK.* , 104–107.

Wu, C., Watanabe, E. & Utsunomiya, T. 1995 An eigenfunction matching method for analyzing the wave induced responses of an elastic floating plate *Appl. Ocean Res.* **17**, 301–310.

Utsunomiya, T., Watanabe, E., Wu, C., Hayashi, N., Nakia, K. & Sekita, K. 1995 Wave response analysis of a flexible floating structure by the BE-FE combination method. *Proc. 5th Int. Offshore and Polar Eng. Conf.* 400–405.

Zilman, G. & Miloh, T. 2000 The diffraction of surface waves by an elastic platform floating on shallow water. *Appl. Ocean Res.* **22**, 191–198.